

1 Analyses of vaccine-specific circulating and bone marrow-
2 resident B cell populations reveal benefit of delayed vaccine
3 booster dosing with blood-stage malaria antigens

4

5 JR Barrett¹, SE Silk¹, CG Mkindi², KM Kwiatkowska¹, MM Hou¹, AM Lias¹, WF Kalinga², IM
6 Mtaka², K McHugh¹, M Bardelli¹, H Davies¹, LDW King¹, NJ Edwards¹, VS Chauhan³, P
7 Mukherji⁴, S Rwezaula⁵, CE Chitnis⁶, AI Olotu², AM Minassian¹, SJ Draper¹, CM Nielsen¹.

8

9 ¹ University of Oxford, Oxford, UK.

10 ² Ifakara Health Institute, Bagamoyo, Tanzania.

11 ³ International Centre for Genetic Engineering and Biotechnology (ICGEB), New Delhi, India.

12 ⁴ Multi Vaccines Development Program (MVDP), New Delhi, India.

13 ⁵ Muhimbili National Hospital, Dar es Salaam, Tanzania.

14 ⁶ Unité de Biologie de Plasmodium et Vaccins, Institut Pasteur, Université Paris Cité, Paris,
15 France.

16

17 Correspondence to: carolyn.nielsen@bioch.ox.ac.uk

18 Abstract

19 We have previously reported primary endpoints of a clinical trial testing two vaccine
20 platforms for delivery of *Plasmodium vivax* malaria DBPRII: viral vectors (ChAd63, MVA) and
21 protein/adjuvant (PvDBPII with 50µg Matrix-M™ adjuvant). Delayed boosting was
22 necessitated due to trial halts during the pandemic and provides an opportunity to
23 investigate the impact of dosing regimens. Here, using flow cytometry – including agnostic
24 definition of B cell populations with the clustering tool CITRUS – we report enhanced
25 induction of DBPRII-specific plasma cell and memory B cell responses in protein/adjuvant
26 versus viral vector vaccinees. Within protein/adjuvant groups, delayed boosting further
27 improved B cell immunogenicity as compared to a monthly boosting regimen. Consistent
28 with this, delayed boosting also drove more durable anti-DBPRII serum IgG. In an
29 independent vaccine clinical trial with the *P. falciparum* malaria RH5.1 protein/adjuvant
30 (50µg Matrix-M™) vaccine candidate, we similarly observed enhanced circulating B cell
31 responses in vaccinees receiving a delayed final booster. Notably, a higher frequency of
32 vaccine-specific (putatively long-lived) plasma cells were detected in the bone marrow of
33 these delayed boosting vaccinees by ELISPOT and correlated strongly with serum IgG.

34

35 Finally, following controlled human malaria infection with *P. vivax* parasites in the DBPRII
36 trial, *in vivo* growth inhibition was observed to correlate with DBPRII-specific B cell and
37 serum IgG responses. In contrast, the CD4+ and CD8+ T cell responses were impacted by
38 vaccine platform but not dosing regimen, and did not correlate with *in vivo* growth inhibition
39 in a challenge model. Taken together, our DBPRII and RH5 data suggest an opportunity for
40 dosing regimen optimisation in the context of rational vaccine development against
41 pathogens where protection is antibody-mediated.

42 Introduction

43 The roll-out of various SARS-CoV-2 vaccines during the COVID-19 pandemic highlighted the
44 importance of understanding the immunological significance of booster dosing timing in
45 order to maximise protective efficacy. Increased peak serum antibody concentrations were
46 observed with delayed booster regimens in both viral vector [1; 2] and mRNA [3] delivery
47 platforms, indicating potential opportunities to maximise humoral immunity through
48 optimisation of antigen delivery timing. The impact of delayed booster regimens has also
49 been explored in more depth by earlier work from the *Plasmodium falciparum* malaria field
50 with both the blood-stage malaria vaccine candidate RH5 [4; 5] and the pre-erythrocytic
51 vaccine candidate RTS,S (now WHO-approved as Mosquirix; [6; 7; 8; 9; 10]). Notably, the
52 impact of delayed booster dosing on vaccine-specific serum IgG durability has been
53 published less widely; the RH5 trials remain the only example of improvements in durability
54 through modifications in booster dosing regimens [4; 5]. We have previously speculated on
55 the underlying biological mechanisms and reasons for discrepancies between the RTS,S
56 and RH5 trials [5], and these questions clearly require further investigation. Furthermore, it is
57 critical to confirm whether the delayed booster phenomenon is a broader immunological
58 principle, or an anomaly restricted to the RH5.1/AS01 vaccine candidate.

59

60 Here, we present analyses of B cell, T cell and serum antibody responses to a blood-stage
61 malaria antigen from a different species of malaria – DBPR11, *Plasmodium vivax* – and
62 investigate the impact of delayed boosters in the context of heterologous viral vector or
63 protein/adjuvant vaccine platforms (**Table 1**). This work builds on the initial clinical trial
64 publication, which focused on the efficacy results of the controlled human malaria infection
65 (CHMI) [11]. Supporting these findings, we additionally present peripheral B cell analyses
66 (using the same B cell flow cytometry panel) from a *P. falciparum* RH5.1/Matrix-M™ vaccine
67 trial where PBMC samples were available for exploratory analyses. For the first time in the

68 context of malaria vaccinology, we also report on vaccine-specific bone marrow plasma
69 cells.

70

71 Taken together, our data support delayed booster vaccination in the next phase of *P. vivax*
72 DBPRII and *P. falciparum* RH5 vaccine development and, more broadly, support
73 consideration of alternative dosing regimens for vaccines against a range of pathogens
74 where protection is antibody-mediated.

75

76 **Table 1. Vaccination regimens in DBPRII and RH5 clinical trials.** Post-vaccination
77 samples analysed in this study are following the final vaccination (FV), indicated by the
78 highlighted cell. See Methods for further details of clinical trial design.

Target	Platform	Dosing regimen	Timing of vaccinations (m = month)				n [§]
			Dose 1	Dose 2	Dose 3	Dose 4	
<i>P. vivax</i> DBPRII	ChAd63- DBPRII and MVA-DBPRII viral vectors	Monthly [VV-M]	0m	2m	-		6
		Delayed [VV-D]	0m	17m	19m		2
	PvDBPII protein/ Matrix-M™	Monthly [PA-M]	0m	1m	2m		4
		Delayed [PA-D]	0m	1m	14m		8
		Delayed + booster [PA-DB]	0m	1m	14m	19m	5
		(Same vaccinees as PA-D)					
<i>P. falciparum</i> RH5	RH5.1 protein/ Matrix-M™	Monthly [M]	0m	1m	2m		5
		Delayed [D]	0m	1m	6m*		6

79 [§] Reflects sample size of groups completing full vaccination regimen in clinical trials [11]. All
80 trial participants were healthy adults. Sample sizes for individual assays are specified in
81 figure legends.

82 * Final dose of antigen (but not adjuvant) in the delayed arm of *P. falciparum* RH5 trial was
83 also fractionated (see Methods).

84 Results

85 Delayed booster dosing increases induction of circulating DBPRII- and RH5-specific
86 plasma cells and memory B cells.

87 Using fluorophore-conjugated DBPRII protein probes to detect DBPRII-specific cells, we
88 evaluated the capacity of the viral vector and protein/adjuvant platforms to drive a range of B
89 cell responses (gating strategy shown in **Supplemental Figure 1A**). Within the plasma cell
90 population (CD19+CD27+CD38+; **Figure 1A**) – which peaked 7-days after final vaccination
91 – significantly higher frequencies of DBPRII-specific cells were observed in protein/adjuvant
92 as compared to heterologous viral vector vaccinees at FV+7 and FV+14. Within the memory
93 IgG+ B cell population (CD19+CD27+IgG+ [excluding plasma cells]; **Figure 1B**), frequencies
94 of DBPRII-specific cells were significantly higher in protein/adjuvant vaccinees at all post-
95 vaccination time points. Consistent with expected differences in kinetics of short-lived
96 plasma cell (SLPC) and memory B cell responses, DBPRII-specific plasma cells peaked
97 earlier at FV+7 and then declined by FV+28, whilst frequencies of DBPRII-specific memory
98 IgG+ B cells were better maintained in peripheral blood between FV+7 and FV+28 (with a
99 trend towards a peak at FV+14 [5]).

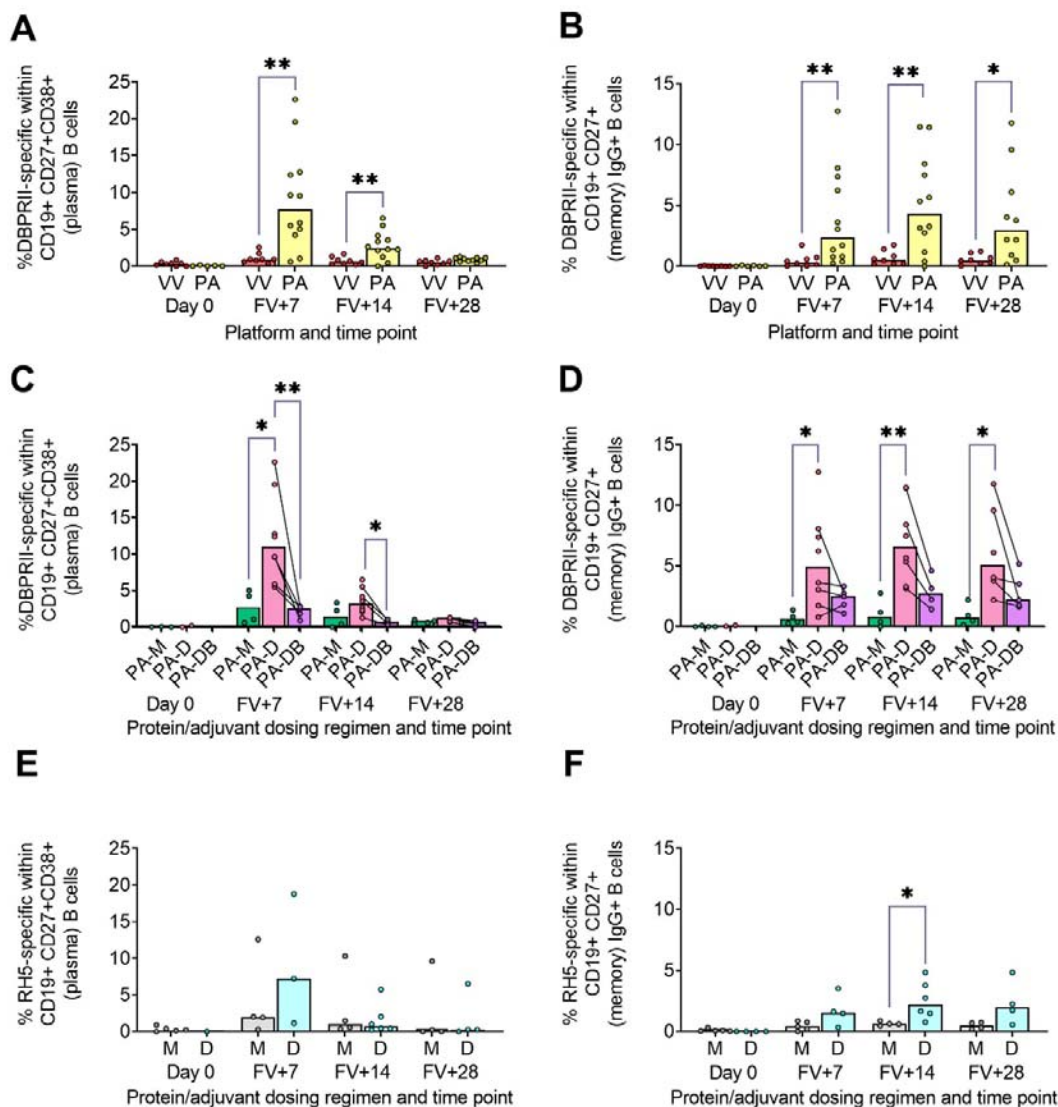
100

101 We next compared DBPRII-responses between the dosing regimens of the protein/adjuvant
102 platform. Here, we observed more robust plasma cell (**Figure 1C**) and memory IgG+ B cell
103 (**Figure 1D**) responses following delayed booster dosing (PA-D) as compared to monthly
104 booster dosing (PA-M). Proliferation – as indicated by intracellular Ki67 staining – was higher
105 in plasma cells than memory B cells across all groups and time points (**Supplemental**
106 **Figure 1B-C**). Differences between platforms and dosing regimens remained when we
107 stratified between activated (CD21-CD27+) and resting (CD21+CD27+) memory IgG+ B cell
108 populations (**Supplemental Figure 2A-D**). Interestingly, Ki67 expression was significantly
109 higher in activated memory IgG+ B cells in PA-D at FV+7 as compared to PA-M or PA-DB,
110 and at FV+14 as compared to PA-M (**Supplemental Figure 1C-D**). Very low memory IgA+ B

111 cell responses were detectable (higher in protein/adjuvant than viral vector vaccinees), while
112 responses within the IgM+ memory compartment were negligible (**Supplemental Figure 2E-**
113 **H**).

114

115 We sought to validate these delayed booster dosing-mediated differences with samples from
116 an independent clinical trial with a different cohort (Tanzanian adults) and antigen (RH5).
117 Here, we observed comparable plasma cell and memory IgG+ B cell kinetics and differences
118 in proliferation (**Figure 1E-F; Supplemental Figure 3**). Frequencies of RH5-specific cells
119 within both populations were again higher in delayed booster dosing vaccinees but only
120 reached statistical significance (by Mann Whitney test) for RH5-specific memory B cells at
121 FV+14, likely related to greater intra-group variation as compared to the DBPRII vaccinees.
122 Trends were comparable, but not significant, when activated and resting memory IgG+ B
123 cells were analysed separately (**Supplemental Figure 4**). To note, while background with
124 the RH5 probes was more variable than observed with the DBPRII probes here, or in
125 previous studies with the RH5 probe protocol [5; 12], standardisation of RH5 probe gating
126 between all samples and parent populations retains confidence in the data interpretation. No
127 significant post-vaccination responses were observed for RH5-specific memory IgA+ or IgM+
128 populations (**Supplemental Figure 4**).



129

130 Figure 1. Vaccinate-specific plasma cell and memory IgG+ B cell responses.

131 PBMC from pre-vaccination (Day 0) and post-final vaccination (FV) time points were analysed for B cell
 132 responses by flow cytometry; gating strategies are as described in Methods and **Supplemental Figures 1 and 3**.
 133 Frequencies of DBPRII-specific B cells – identified by probe staining – were compared between vaccine
 134 platforms (A-B) or protein/adjuvant dosing regimens (C-D) within both plasma cell (A, C) or memory IgG+ B cell
 135 (B, D) populations. Similarly, frequencies of RH5-specific B cells were compared between protein/adjuvant
 136 dosing regimens within plasma cell (E) and memory IgG+ B cells (F). IgM+, IgA+, activated and resting memory
 137 B cell responses are shown in **Supplemental Figures 2 and 4**. VV = ChAd63-MVA viral vectors; PA = PvDBP
 138 protein/adjuvant [PA-M and PA-D]; PA-M = PvDBP protein/adjuvant monthly dosing; PA-D = PvDBP
 139 protein/adjuvant delayed booster dosing; PA-DB = PvDBP protein/adjuvant delayed booster dosing with extra
 140 booster; M = RH5.1/adjuvant monthly dosing; D = RH5.1/adjuvant delayed booster dosing. Post-vaccination
 141 comparisons were performed between DBPRII platforms (A-B) or RH5 dosing regimens (E-F) with Mann-Whitney
 142 U tests, or between PvDBP protein/adjuvant dosing regimens by Kruskal Wallis test with Dunn's correction for
 143 multiple comparisons (C-D). Sample sizes for all assays were based on sample availability; each circle
 144 represents a single sample. (A-B) VV/PA: Day 0 = 8/5-6, FV+7 = 8/12, FV+14 = 8/12, FV+28 = 8/10. (C-D) PA-
 145 M/PA-D/PA-DB: Day 0 = 3-4/2/na, FV+7 = 4/8/5, FV+14 = 4/8/4, FV+28 = 4/6/5. (E-F) M/D: Day 0 = 5/1-4, FV+7
 146 = 4-5/3-4, FV+14 = 4/6, FV+28 = 4/4. PA-D vaccinees returning in the PA-DB group are connected by lines. Bars
 147 represent medians. * $p < 0.05$, ** $p < 0.01$.

148 Agnostically-defined B cell subsets reveal further differences in DBPRII- and RH5-
 149 specific B cell responses between vaccine platforms and dosing regimens

150 To supplement the more traditional approach above, clustering was next performed with
 151 CITRUS to agnostically define B cell populations for further analysis within both the DBPRII
 152 and RH5 datasets. For the DBPRII trial samples, 33 clusters were identified in CITRUS
 153 within live single (B cell-enriched) lymphocytes. Several sets of clusters had very similar
 154 marker expression patterns, resulting in consolidation for FlowJo gating strategies (see
 155 Methods). This gave a total of 7 agnostically-defined populations to reanalyse for DBPRII-
 156 specific responses (**Table 2**). Likewise, 36 clusters were identified in the RH5 trial samples,
 157 consolidating to 10 new populations for reanalysis of RH5-specific responses (**Table 2**).
 158 Populations where significant differences in antigen-specific responses were detected post-
 159 vaccination or between dosing regimens are shown in **Figure 2** (gating shown in
 160 **Supplemental Figure 5**). DBPRII “Population 2” and RH5 “Population 8” were equivalent,
 161 while all other populations identified were unique to the separate trials.

162

163 **Table 2. Main peripheral B cell populations as agnostically defined using CITRUS.** NB
 164 population ordering and numbers are arbitrary.

Trial	Population	FlowJo gating strategy						
		CD19	CD20	CD21	CD27	CD138	CD38	Isotype
DBPRII	1*	+	+	+	+	-	-	IgG
	2* [%]	-	-	-	-	-	+	IgG
	3	+	+	+	-	-	-	IgM
	4	-	-	-	-	-	-	IgG
	5	+	+	+	+	-	-	IgA
	6	+	+	+	-	+	-	IgM
	7	+	+	+	+	-	-	IgM
RH5	8 [%]	-	-	-	-	-	+	IgG
	9	-	-	-	+	-	+	IgG
	10	+	+	+	-	-	+	IgM
	11	+	+	+	+	-	+	IgM
	12*	+	+	+	+	-	+	IgG
	13	+	+	+	+	-	+	IgA
	14	+	+	+	-	+	+	IgM
	15	-	-	-	-	-	-	-
	16	+	+	+	-	-	+	IgA
	17	+	+	+	-	-	+	-

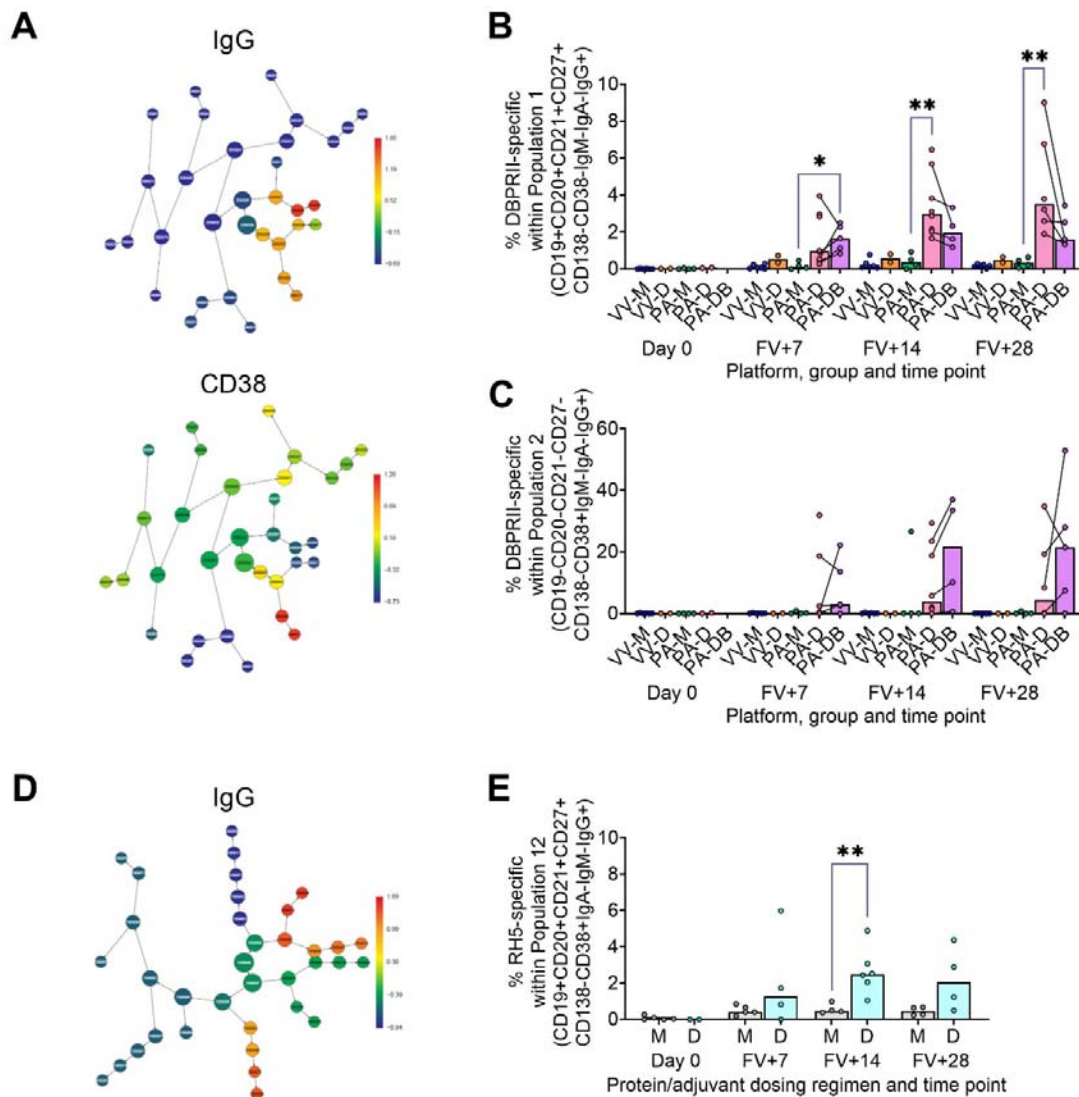
165 * Significant antigen-specific responses detected within groups; shown in **Figure 2**; gating strategies shown in
 166 **Supplemental Figure 5**. [%] Equivalent populations identified independently.

167

168 In the DBPRII trial clusters, significant differences were observed between monthly and
169 delayed dosing in “Population 1” (CD19+CD20+CD21+CD27+CD138-CD38-IgM-IgA-IgG+;
170 **Figure 2B; Supplemental Figure 5**) and trends between monthly and delayed or
171 delayed/booster (PA-DB) dosing in “Population 2” (CD19-CD20-CD21-CD27-CD138-
172 CD38+IgM-IgA-IgG+; **Figure 2C; Supplemental Figure 5**). While “Population 1” is similar to
173 the CD19+CD21+CD27+IgG+ resting memory population analysed above (**Supplemental**
174 **Figure 2**), Population 2 was not included in the previous analysis. Responses within other
175 clusters and frequencies of each cluster within total live (B cell-enriched) lymphocytes are
176 shown in **Supplemental Figure 6**.

177

178 In the new RH5 trial populations, significant responses were observed in Population 12
179 (**Figure 2E; Supplemental Figure 5**; CD19+CD20+CD21+CD27+CD138-CD38+IgM-IgA-
180 IgG+; again, a similar population to CD19+CD27+IgG+ in **Figure 1F**) in both monthly and
181 delayed booster dosing, with higher responses in delayed boosting vaccinees. Significant
182 differences in post-vaccination RH5-specific responses were not detected between groups in
183 the remaining populations (**Supplemental Figure 7**). No significant responses were
184 observed within Population 8 (CD19-CD20-CD21-CD27-CD138-CD38+IgM-IgA-IgG+;
185 equivalent Population 2 in the DBPRII trial) in the delayed boosting vaccinees.

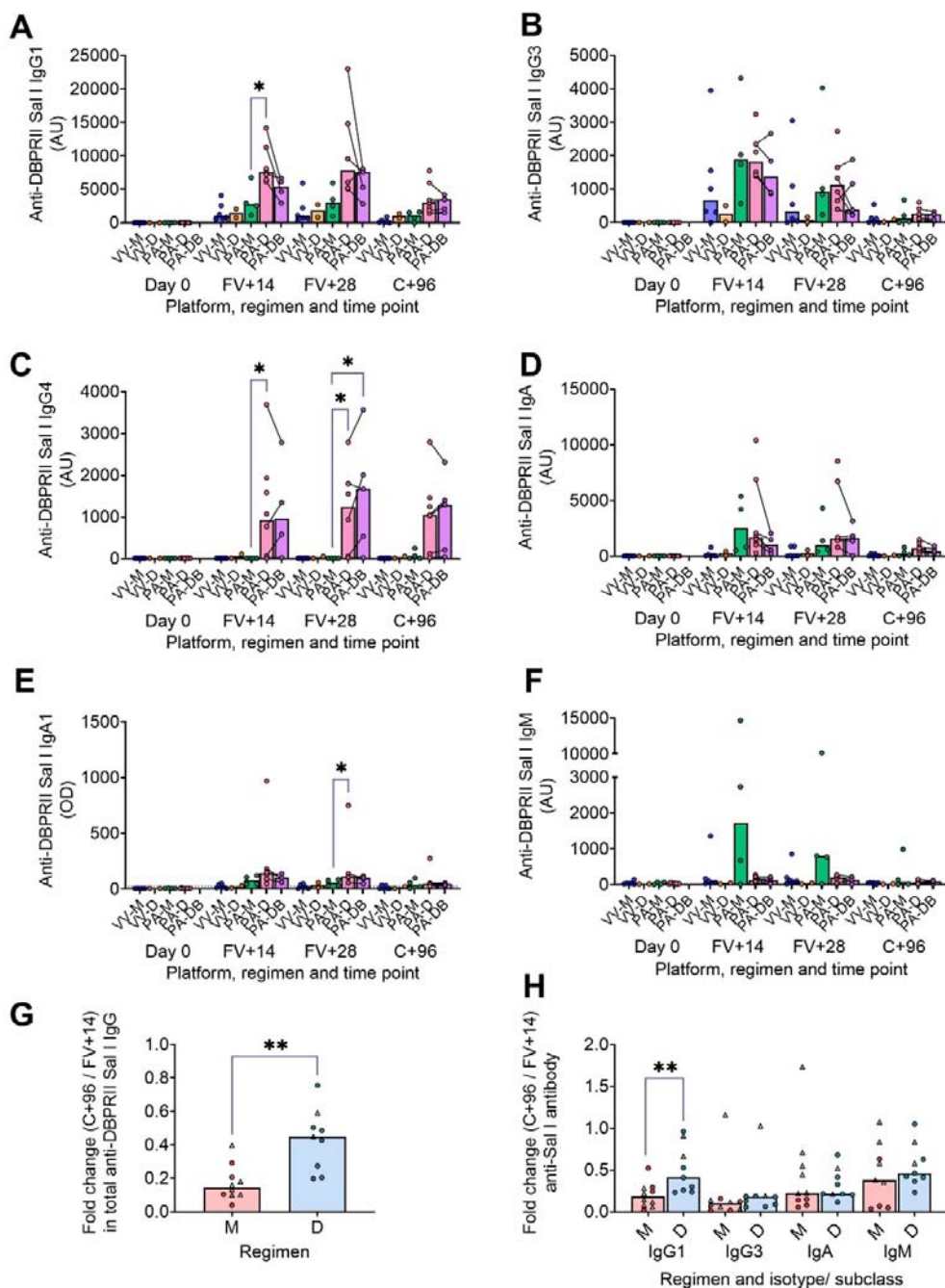


186

187 Figure 2. Vaccine-specific responses within agnostically-defined B cell populations using CITRUS.
 188 CITRUS was run on single live (B cell-enriched) lymphocyte flow cytometry fcs files to agnostically define the
 189 main B cell populations within either DBPR11 (A-C) or RH5 (D-E) trial samples. Clusters identified by CITRUS are
 190 visualised in dendrograms (A, D), colour-coded for example markers of interest (A- IgG, CD38; D- IgG). Each
 191 node represents a cluster. Median marker expression within each cluster was used to define gating strategies for
 192 B cell populations in FlowJo, which were re-analysed for DBPR11- (B-C) or RH5-specific (E) responses through
 193 probe staining (gating shown in Supplemental Figure 5). See Table 2 and Supplemental Figures 6-7 for a full
 194 list of populations identified via CITRUS clusters for further analysis. VV-M = ChAd63-MVA viral vector monthly
 195 dosing; VV-D ChAd63-MVA delayed booster dosing; PA-M = PvDBP11 protein/adjuvant monthly dosing; PA-D =
 196 PvDBP11 protein/adjuvant delayed booster dosing; PA-DB = PvDBP11 protein/adjuvant delayed booster dosing
 197 with extra booster; M = RH5.1/adjuvant monthly dosing; D = RH5.1/adjuvant delayed booster dosing. FV = final
 198 vaccination. Post-vaccination comparisons were performed between PvDBP11 protein/adjuvant dosing regimens
 199 by Kruskal Wallis test with Dunn's correction for multiple comparisons (B-C) or RH5 dosing regimens (E) with
 200 Mann-Whitney U tests. Sample sizes for all assays were based on sample availability; each circle represents a
 201 single sample. (B-C) VV-M/VV-D/PA-M/PA-D/PA-DB: Day 0 = 6/2/4/2/na, FV+7 = 6/2/4/8/5, FV+14 = 6/2/4/8/4,
 202 FV+28 = 6/2/4/6/5. (E) M/D: Day 0 = 5/2, FV+7 = 5/4, FV+14 = 4/6, FV+28 = 4/4. PA-D vaccinees returning in the
 203 PA-DB group are connected by lines. Bars represent medians. * $p < 0.05$, ** $p < 0.01$.

204 DBPRII-specific serum antibody declines more slowly in delayed booster dosing
205 vaccinees.

206 We have previously published ELISA data on serum anti-DBPRII total IgG (against the Sal I
207 strain), with an emphasis on comparison of FV+14 responses. Here we observed
208 significantly higher titres with the delayed protein/adjuvant dosing regimen as compared to
209 viral vectors [11]. Now, we extend these analyses to compare the impact of platform and
210 regimen on different isotypes/ subclasses, (**Figure 3A-F; Supplemental Figure 8**), durability
211 of serum antibody (**Figure 3G-H**), and immunodominance of subdomain 3 (sd3;
212 **Supplemental Figure 8**). The isotype and subclass analyses showed IgG1, IgG3, IgA and
213 IgA1 responses in both platforms, while IgG4 was detectable solely in the protein/adjuvant
214 vaccinees. No statistically significant post-vaccination IgM responses were observed within
215 individual groups (**Supplemental Figure 8**), while no detectable IgG2 or IgA2 was observed
216 in any sample (not shown). The protein/adjuvant platform also induced higher IgG1, IgG3,
217 IgA and IgA1 (and IgG4) responses as compared to viral vectors (**Supplemental Figure 8A-**
218 **F**). Within the protein/adjuvant platform, the DBPRII-specific IgG1, IgG4 and IgA1 response
219 was significantly higher in delayed dosing vaccinees (**Figure 3A, C, E**), but comparable
220 between regimens for IgG3 and IgA (**Figure 3B, D**). Median IgM responses were higher in
221 monthly dosing but not statistically significant (**Figure 3F**). Interestingly, we also observed
222 increased anti-DBPRII serum total IgG durability in delayed dosing regimens with both
223 vaccine platforms; a significantly higher fold-change in total serum IgG was observed > 3-
224 months following the peak response in delayed booster vaccinees (VV-D, PA-D; median =
225 0.45) as compared to monthly dosing vaccinees (VV-M, PA-M; median = 0.15; **Figure 3G**).
226 Enhanced serum durability was also observed with IgG1 in the isotype and subclass
227 analyses (**Figure 3H**). Finally, delayed dosing with PvDBPRII appears to have no impact on
228 the immunodominance of the sd3 region (**Supplemental Figure 8**). Equivalent serological
229 analyses from the RH5.1/Matrix-MTM trial will be the focus of a separate report (Silk et al,
230 *manuscript in preparation*).



231
232
233
234
235
236
237
238
239
240
241
242
243
244
245
246
247

Figure 3. DBPRII-specific peak antibody responses and serum maintenance.

Standardised ELISAs were developed to report anti-DBPRII specific antibody responses against the Sal I strain in pre-vaccination (Day 0) and post-final vaccination (FV) serum samples. Responses were compared between protein/adjuvant dosing regimens for IgG1 (A), IgG3 (B), IgG4 (C), IgA (D), IgA1 (E), and IgM (F). Fold change between C+96 and FV+14 was calculated for total IgG (G) and specific isotypes/subclasses (H) to compare monthly (M: VV-M, PA-M) and delayed (D: VV-D, PA-D) booster regimens. IgG4 and IgA were excluded from this analysis as ≥ 1 vaccinee had undetectable antibody at both time points. Comparisons between vaccine platforms are shown in **Supplemental Figure 8**. VV-M = ChAd63-MVA viral vector monthly dosing; VV-D = ChAd63-MVA delayed booster dosing; PA-M = protein/adjuvant monthly dosing; PA-D = protein/adjuvant delayed booster dosing; PA-DB = protein/adjuvant delayed booster dosing with extra booster. C+96 = 96 days after controlled human malaria infection (approximately 16-weeks after FV). Post-vaccination comparisons were performed between protein/adjuvant dosing regimens by Kruskal Wallis test with Dunn's correction for multiple comparisons (A-F) or fold changes with Mann-Whitney U tests (G-H). Sample sizes for all assays were based on sample availability; each circle represents a single sample [triangles indicate viral vector samples in G-H]. (A-F) VV-M/VV-D/PA-M/PA-D/PA-DB: Day 0 = 6/2/4/8/na, FV+14 = 6/2/4/8/4, FV+28 = 6/2/4/6/5. (G-H) M = 9-10, D = 9. Bars represent medians. * $p < 0.05$, ** $p < 0.01$.

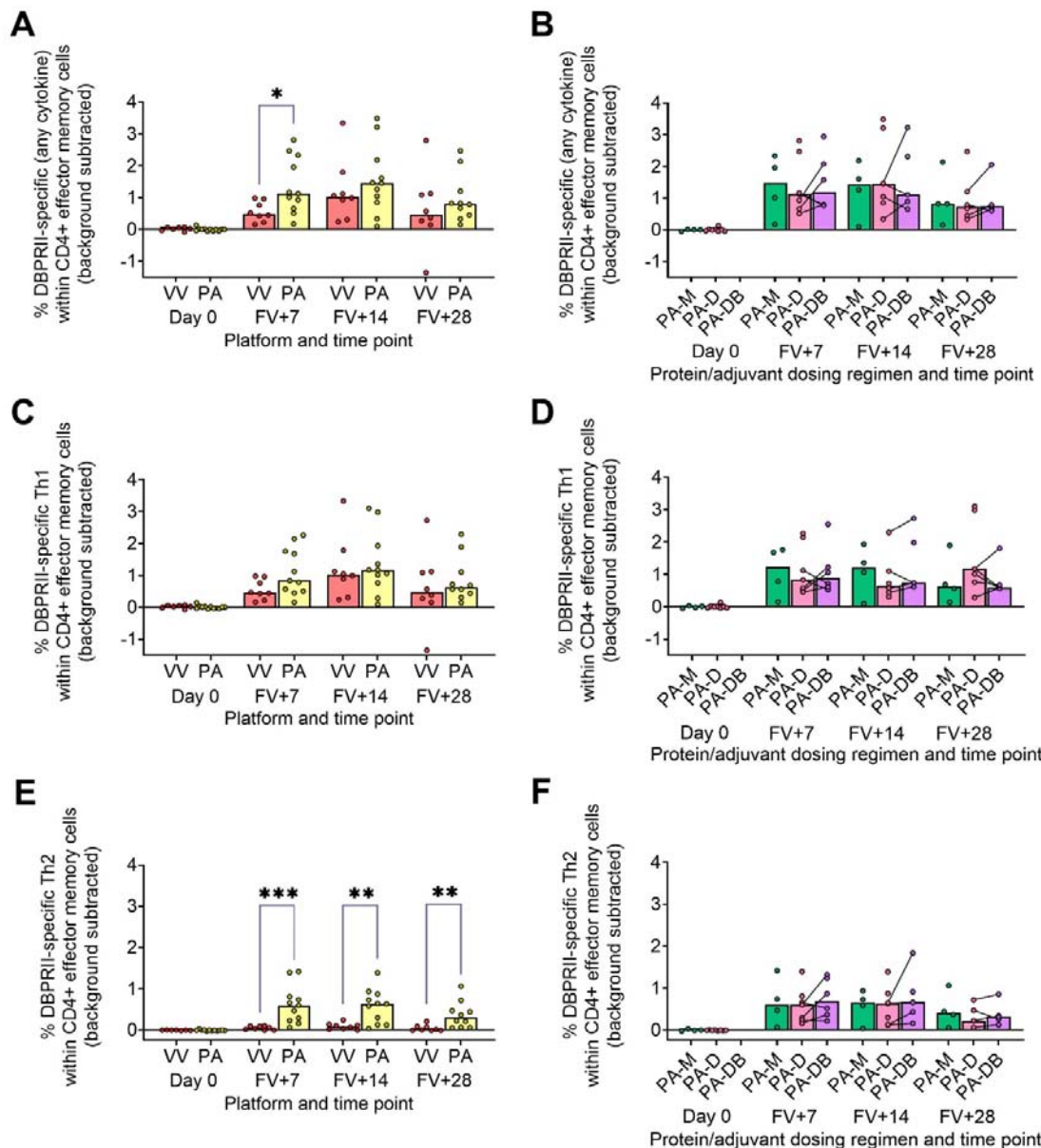
248 Delayed booster dosing does not impact DBPRII-specific T cell responses

249 In our main trial report, we showed higher frequencies of IFN- γ -producing effector memory
250 (CD45RA-CCR7-) CD4+ T cells at FV+14 in viral vector as compared to protein/adjuvant
251 vaccinees, with no significant differences observed between monthly and delayed dosing
252 regimens with the latter platform [11]. Here, we extended these analyses to include further
253 time points as well as IL-2/ TNF- α / IL-5/ IL-13 intracellular cytokine detection (in addition to
254 IFN- γ), allowing a more nuanced comparison of responses between vaccine platform and
255 regimen. Looking first at all DBPRII-specific effector memory CD4+ T cells – based on
256 secretion of any cytokine following stimulation with the DBPRII peptide pool (**Table 3**) – we
257 observed significantly higher frequencies in protein/adjuvant vaccinees at FV+7 as
258 compared to viral vector vaccinees, but no difference between dosing regimens (**Figure 4A-**
259 **B**). Within the same effector memory CD4+ T cell population, we next assessed total Th1
260 (defined as IFN- γ and/or IL-2 and/or TNF- α) and Th2 responses (IL-5 and/or IL-13). Both
261 platforms induced Th1 cytokine production and there were no significant differences
262 between platforms or dosing regimens (**Figure 4C-D**). In contrast, the protein/adjuvant
263 vaccines drove higher frequency Th2 responses, comparable across different dosing
264 regimens (**Figure 4E-F**). Trends were similar for both IL-5 and IL-13, although the magnitude
265 of DBPRII-specific IL-5-producing cells was higher (median [range] % DBPRII-specific cells
266 within effector memory CD4+ T cells at FV+7: VV IL-5 = 0.04% [0.00-0.10%], PA IL-5 =
267 0.60% [0.06-1.35%]; IL-13 VV 0.02% [0.00-0.06%], PA IL-13 = 0.06% [0.02-0.42%]).

268

269 Finally, we similarly quantified the effector memory CD8+ T cell response. Here, higher IFN-
270 γ responses were observed with the viral vector platform; no significant responses were
271 observed within the protein/adjuvant platform (**Supplemental Figure 9**).

272



273

274

Figure 4. DBPRII-specific CD4+ effector memory T cell responses.

275

PBMC from pre-vaccination (Day 0) and post-final vaccination (FV) time points were analysed for T cell

276

responses by intracellular cytokine staining; gating strategies are as described in Methods and **Supplemental**

277

Figure 9. In brief, DBPRII-specific effector memory CD4+ T cells are reported as frequencies producing

278

cytokines in response to peptide stimulation after background subtraction of cytokine-positive cells in matched

279

samples cultured with media alone. DBPRII-specific responses were compared between vaccine platforms or

280

protein/adjuvant dosing regimens as defined by production of any cytokine [IL-2, IL-5, IL-13, IFN- γ , TNF- α] (**A-B**),

281

any Th1 cytokine [IL-2, IFN- γ , TNF- α] (**C-D**), or any Th2 cytokine [IL-5, IL-13] (**E-F**). CD8+ effector memory T cell

282

responses are shown in **Supplemental Figure 9**. VV = ChAd63-MVA viral vectors; PA = PvDBPII

283

protein/adjuvant [PA-M and PA-D]; PA-M = PvDBPII protein/adjuvant monthly dosing; PA-D = PvDBPII

284

protein/adjuvant delayed booster dosing; PA-DB = PvDBPII protein/adjuvant delayed booster dosing with extra

285

booster. Post-vaccination comparisons were performed between PvDBPII platforms by Mann Whitney U test (**A**,

286

C, **E**), or protein/adjuvant dosing regimens by Kruskal Wallis test with Dunn's correction for multiple comparisons

287

(**B**, **D**, **F**). Sample sizes for all assays were based on sample availability; each circle represents a single sample.

288

(**A**, **C**, **E**) VV/PA: Day 0 = 7/12, FV+7 = 8/11, FV+14 = 8/11, FV+28 = 8/10. (**B**, **D**, **E**) PA-M/PA-D/PA-DB: Day 0 =

289

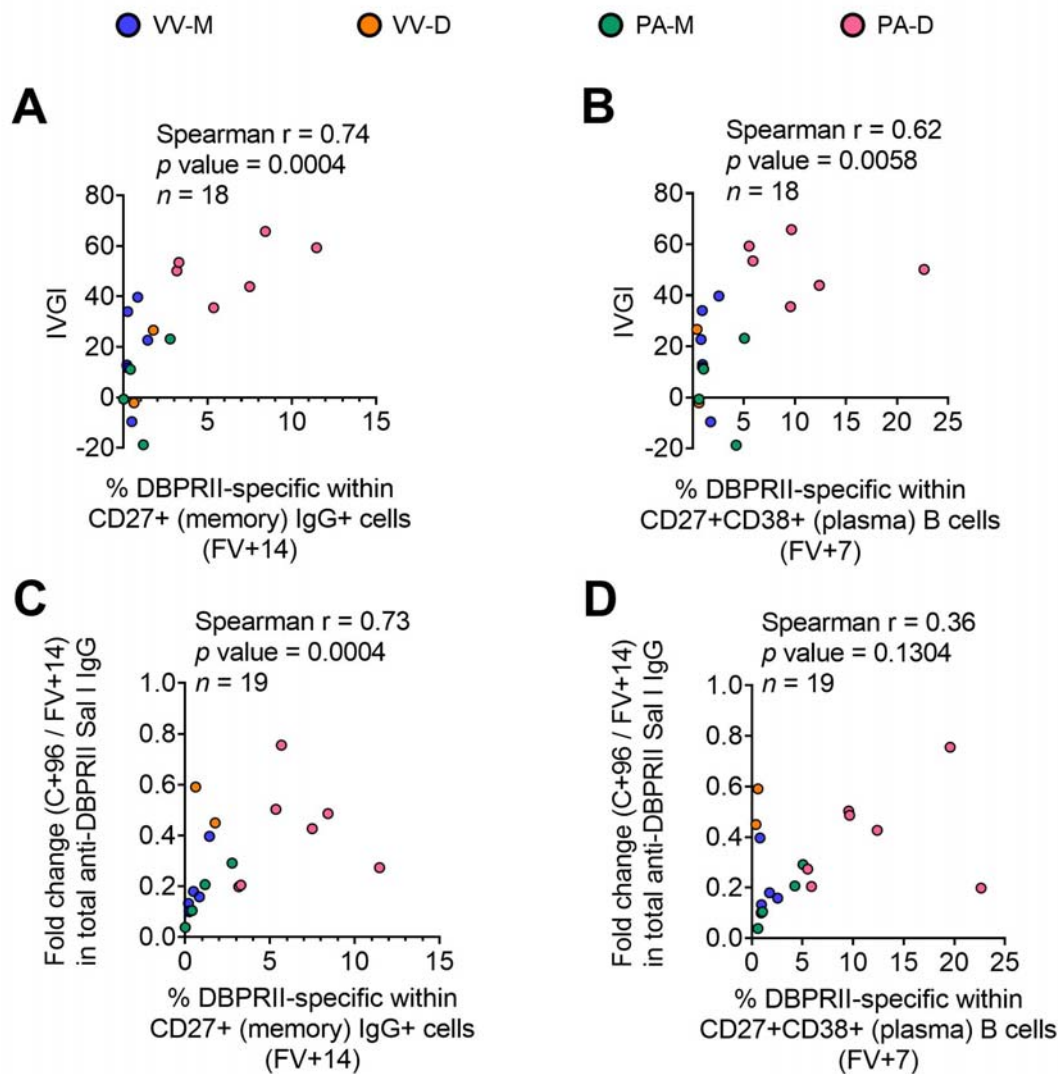
4/8/na, FV+7 = 4/7/6, FV+14 = 4/7/5, FV+28 = 4/6/5. PA-D vaccinees returning in the PA-DB group are

290

connected by lines. Bars represent medians. * $p < 0.05$, ** $p < 0.01$, *** $p < 0.001$.

291 DBPRII-specific B cell responses correlate with *in vivo* efficacy against *P. vivax*
292 parasites and durability of anti-DBPRII serum IgG

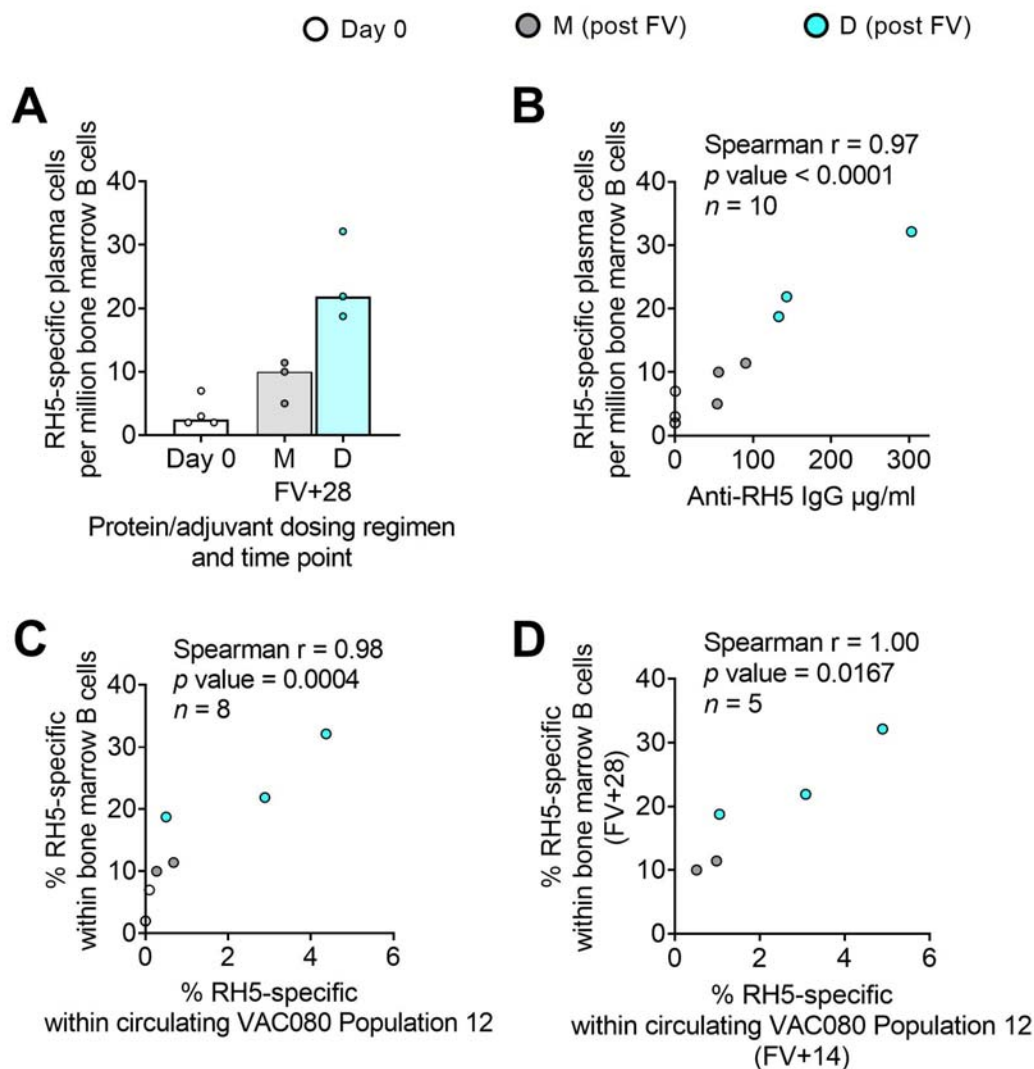
293 To confirm the biological relevance of increased B cell immunogenicity in delayed dosing
294 vaccinees we performed Spearman correlations with *in vivo* growth inhibition of blood-stage
295 parasites following *P. vivax* CHMI [11]. The magnitude of the circulating DBPRII-specific
296 memory IgG+ B cell response correlated strongly with IVGI (**Figure 5A**), as did the
297 frequency of DBPRII-specific plasma cells (**Figure 5B**). Since IVGI is calculated over a
298 relatively short time frame following parasite inoculation, we were also interested in
299 assessing the relationship between these B cell responses and the fold change in serum
300 antibody between the peak (FV+14) and a later time point (C+96, approximately 16-weeks
301 later; **Figure 3G**). DBPRII-specific IgG+ memory B cells again correlated strongly with
302 durable serum anti-DBPRII IgG responses (**Figure 5C**), while no association was observed
303 with peak FV+7 plasma cells (**Figure 5D**). Neither IVGI nor serum antibody maintenance
304 correlated with DBPRII-specific Th2 effector memory CD4+ T cell responses (data not
305 shown), suggesting a lesser role for T cell immunogenicity in DBPRII vaccine-mediated
306 protection.



307
 308 Figure 5. Correlations between circulating DBPRII-specific B cells and *in vivo* growth inhibition of *P.*
 309 *vivax* parasites or maintenance of serum antibody.
 310 *In vivo* growth inhibition (IVGI) of *P. vivax* parasites following post-vaccination controlled human malaria infection
 311 (CHMI) was calculated from qPCR data as described in the Methods. Spearman correlations were performed
 312 between IVGI and the peak frequency of DBPRII-specific memory IgG+ B cells at FV+14 (A) or plasma cells at
 313 FV+7 (B) as defined in **Supplemental Figure 1** and reported in **Figure 1**. Spearman correlations were also
 314 performed between C+96/FV+14 fold change in total anti-DBPRII IgG (Sal I strain; see **Figure 3**) and memory
 315 IgG+ B cells at FV+14 (C) or plasma cell at FV+28 (D). VV-M = ChAd63-MVA viral vector monthly dosing; VV-D
 316 ChAd63-MVA delayed booster dosing; PA-M = protein/adjuvant monthly dosing; PA-D = protein/adjuvant delayed
 317 booster dosing. C+96 = 96 days after controlled human malaria infection (approximately 16-weeks after FV).
 318 Spearman rho, p values and sample sizes are annotated on individual graphs. Each circle represents a single
 319 sample.

320 Bone marrow plasma cells correlate with serum antibody and circulating memory B
321 cells in adult RH5.1/Matrix-MTM vaccinees

322 While bone marrow aspirates were not taken in the DBPRII clinical trials, we had the rare
323 opportunity to investigate bone marrow plasma cells with the RH5.1/Matrix-MTM adult
324 vaccinees – the first bone marrow analyses in the context of malaria vaccination [13]. Here,
325 we observed a trend to higher frequencies of RH5-specific cells within total bone marrow B
326 cells in the delayed dosing regimen (**Figure 6A**) which correlated strongly with matched time
327 point serum anti-RH5 IgG (**Figure 6B**). We were also interested to see if the frequencies of
328 RH5-specific cells within circulating B cell populations of interest correlated with vaccine-
329 specific seeding of the bone marrow. We therefore performed additional Spearman
330 correlation analyses between the frequency of RH5-specific cells within “Population 12”
331 (CD19+CD20+CD21+CD27+ CD138-CD38+IgA-IgM-IgG+; the B cell population with
332 greatest differences between regimens) at both matched time points (i.e. V1 or FV+28;
333 **Figure 6C**) or with FV+14 (**Figure 6D**). We observe strong correlations between RH5-
334 specific circulating memory B cells and bone marrow plasma cells at both time points.
335 Similar results were obtained if correlations were performed with RH5-specific
336 CD19+CD27+IgG+ B cells (**Figure 1F**; data not shown). RH5-specific bone marrow B cells
337 did not correlate with circulating RH5-specific CD27+CD38+ (plasma) cells at FV+7 (data not
338 shown).



339
 340
 341
 342
 343
 344
 345
 346
 347
 348
 349
 350
 351
 352

Figure 6. RH5-specific bone marrow plasma cell responses and correlations with serum antibody or circulating RH5-specific cells.

RH5-specific bone marrow plasma cells were detected in B cells enriched from pre- and post-final vaccination (FV) bone marrow mononuclear cells and assayed by IgG antibody-secreting cell ELISPOT as described in the Methods. The frequency of RH5-specific IgG plasma cell (antibody-secreting cell) per million bone marrow B cells was compared between dosing regimens (A). Spearman correlation analyses were performed between RH5-specific bone marrow B cells and matched time point serum IgG (B), matched time point frequency of RH5-specific cells within CITRUS-guided “Population 12” [CD19+CD20+CD21+CD27+CD138- CD38+IgM-IgA-IgG+; see Table 2, Figure 2, Supplemental Figure 5] (C), and between RH5-specific bone marrow B cells at FV+28 and Population 12 at FV+14 (D). M = RH5.1/adjuvant monthly dosing; D = RH5.1/adjuvant delayed booster dosing. Post-vaccination comparisons were performed between dosing regimens by Mann Whitney U test (A; not significant). Spearman rho, p values and sample sizes are annotated on individual graphs. Each circle represents a single sample.

353 Discussion

354 The data presented here contribute to growing efforts seeking to understand the impact of
355 modifiable vaccine delivery parameters – i.e. vaccine platform or dosing regimen – on
356 protective immune responses. Using samples from independent clinical trials with the blood-
357 stage malaria antigens DBPRII and RH5, we observe a hierarchy of serum antibody and B
358 cell immunogenicity from heterologous viral vectors to monthly protein/adjuvant booster
359 dosing to delayed booster protein/adjuvant vaccination. Consistent with a role for vaccine-
360 specific B cells in sustained humoral immunity, circulating plasma or memory B cell
361 responses correlate with available *in vivo* growth inhibition (IVGI) and durable serum IgG
362 data from the DBPRII trial. In fact, DBPRII-specific memory IgG+ B cells correlate more
363 strongly with IVGI than our previously reported associations between IVGI and serum anti-
364 DBPRII IgG, DARC (the DBP ligand) binding inhibition, or *in vitro* growth inhibitory activity
365 (GIA) with a transgenic *P. knowlesi* strain expressing *P. vivax* DBPRII [11]). In contrast,
366 while differences in CD4+ and CD8+ T cell responses are observed between platforms by
367 intracellular cytokine staining (ICS), there are no discernible differences between
368 protein/adjuvant dosing regimens and no correlation is observed between IVGI and T cell
369 immunogenicity [11].

370

371 Our conclusions are in line with data published by Payne *et al.* showing an increase in
372 SARS-CoV-2 spike-specific IgG+ antibody-secreting B cells by ELISPOT 4-weeks after the
373 second dose with longer intervals between BNT162b2 mRNA doses in naïve vaccinees
374 (median = 3.4 weeks, versus median = 10.1 weeks). More mixed results were observed with
375 T cell immunogenicity. For example, the authors observed decreased spike-specific IFN- γ
376 ELISPOT responses and CD8+ IFN- γ by ICS, alongside increased spike-specific CD4+ IL-2
377 and IFN- γ by ICS [3]). Likewise, recent work from Nicolas *et al.* reported “long interval” (i.e.
378 delayed) booster dosing increases circulating SARS-CoV-2 RBD-specific IgG+ B cells 1-3
379 weeks after the second mRNA dose, without driving major differences in memory CD4+ or

380 CD8+ T cells (as measured by activation-induced marker [AIM] or ICS [14]). Our own
381 previously published work with a similar AIM assay in the context of a UK RH5.1/AS01
382 Phase I vaccine trial showed no effect of delayed boosting on the magnitude of the Tfh cell
383 response, but we did detect a slight shift towards a Tfh2 phenotype as compared to monthly
384 boosting vaccinees [4]. To note, the Nicolas *et al.* study compared “short” (median = 3.0
385 weeks) and “long” (median = 15.8 weeks) intervals between the two mRNA doses similar to
386 the spacing between 2nd and 3rd doses in the RH5 and CSP (RTS,S) trials. However, for
387 many comparisons of parameters between the malaria and SARS-CoV-2 fields it is
388 important to remember that the “delay” is often less substantial in SARS-CoV-2 trials (i.e. a
389 few weeks [1; 2; 3], rather than several months as tested with DBPRII/ RH5/ CSP- based
390 vaccines [4; 5; 6; 7; 8; 9; 11]). We are far from understanding the optimal spacing of booster
391 doses, but if the benefit to B cell immunogenicity with delayed booster vaccination relates to
392 allowing circulating antibody and/or ongoing germinal centres to wane – as we have
393 previously proposed [5] – then it seems likely that this difference of weeks versus months will
394 be immunologically relevant.

395

396 Our approach to the B cell flow cytometry analyses also incorporated an agnostic approach
397 to identifying the main circulating B cells populations through use of the CITRUS clustering
398 tool. Significant post-vaccination responses were observed within DBPRII “Population 1” and
399 RH5 “Population 12”, which appear to be subsets of the resting memory populations.
400 Interestingly, within the DBPRII trial, substantial post-vaccination responses within the
401 protein/adjuvant delayed boosting groups were detected in a new “Population 2” (CD19-
402 CD20-CD21-CD27-CD138-CD38+IgM-IgA-IgG+). This was an unexpected observation that
403 would have been missed with traditional B cell analytical approaches that start from the
404 premise that all B cells are CD19+. Given our flow cytometry assay includes a negative pan
405 B cell enrichment step and IgG expression is not expected on other lymphocytes, it is likely
406 that the vast majority of these CD38+IgG+ cells are true B cells. At present, there appears to
407 be limited and conflicting published data on similar (healthy) human vaccine-specific CD19-

408 B cells in circulation. For example, Arumugakani *et al.* have reported on influenza-specific
409 IgG-secreting CD19-CD20-CD38hi cells by ELISPOT and concluded this population was at
410 the plasmablast to mature plasma cell transition, but in contrast to our “Population 2” data
411 this population was also CD27hi [15]. Conversely, Mei *et al.* did not detect post-vaccination
412 tetanus-toxoid specific cells within circulating CD19-CD38+IgG+ B cells by intracellular
413 probe staining and concluded plasma cell CD19 downregulation does not occur until *in situ*
414 in the bone marrow [16].

415

416 In light of the interest in CD19- B cells in the context of long-lived plasma cell responses
417 future trials with larger sample sizes should include immunokinetic investigations of CD19-
418 subpopulations and their biological significance. Indeed, of great interest is the strong
419 correlation detected between circulating serum IgG or memory B cells and vaccine-specific
420 bone marrow plasma cells in the RH5 trial. Very few vaccine studies have included lymphoid
421 tissue sampling (reviewed in [13]) and, to the best of our knowledge, this trial represents the
422 first direct analysis of human bone marrow-resident plasma cells in the context of malaria.
423 Since long-term serum antibody is maintained through secretion by long-lived plasma cells in
424 the bone marrow, understanding the factors that impact this compartment is central to
425 optimising durability of humoral immunity. Our data strongly suggest that delayed dosing
426 improves seeding of bone marrow plasma cells, as compared to monthly booster dosing.
427 Future studies should build on these exciting findings with larger sample sizes or sample
428 volumes, which would permit more detailed analyses of populations of interest such as the
429 putative long-lived plasma cell population (CD19-CD38+CD138+ [16; 17; 18]) within total
430 bone marrow plasma cells.

431

432 There are also several aspects of the DBPRII serology data that deserve further comment.
433 Firstly, it is interesting to note that median peak responses after an additional booster
434 vaccination (PA-DB vs PA-D) are lower across the majority of isotypes and subclasses
435 measured. This is mirrored in the DBPRII-specific B cell data and indeed reaches statistical

436 significance for the CD27+CD38+ plasma cell response. The exception is serum IgG4 which
437 trends to a higher peak concentration following PA-DB as compared to the PA-D regimen,
438 and in fact we have previously observed an enhanced IgG4 response with higher antigen
439 doses of RH5.1/AS01 in an equivalent UK population [5]. Secondly, we were surprised by
440 the absence of detectable IgG2 following vaccination with any of the platform/ regimens.
441 This is in contrast to the previous RH5 analyses where we observed a (low) IgG2 response
442 to both monthly and delayed booster dosing regimens, with better serum maintenance in the
443 latter group [5]. Finally, while intragroup variation and small sample sizes reduced the
444 statistical power to detect differences in the IgM analyses, it is interesting to note that
445 median responses were higher in the monthly as compared to delayed dosing regimens
446 (FV+14: PA-M = 1708 AU, PA-D = 119.8 AU, PA-DB = 126.0 AU; FV+28: PA-M = 794.1 AU,
447 PA-D = 204.4 AU, PA-DB = 129.4 AU). Although frequencies of DBPRII-specific B cells
448 within the memory IgM+ population were very low, these did trend to slightly higher medians
449 at FV+28 and correlate with serum IgM (Spearman $r = 0.69$, $p = 0.0014$, $n = 18$).

450

451 Given the multitude of parameters assayed, machine learning – such as with the SIMON
452 platform [19] – would have been a useful strategy for interrogating which read-out or set of
453 read-outs best predicted our trial outcomes of interest e.g. peak vaccine-specific IgG, IVGI
454 (DBPRII trial only) or seeding of bone marrow plasma cells (RH5 trial only). Unfortunately,
455 this approach was precluded by insufficient sample size. Indeed, the small sample sizes of
456 the different vaccination groups represents the main limitation of our analyses for both trials.

457

458 To conclude, our data indicate that while changing vaccine platform drives broad effects on
459 post-vaccination immune responses, modulating booster dosing regimen more narrowly
460 impacts humoral immunity. Importantly, these differences in immunogenicity appear to have
461 relevance for protection from *P. vivax* in a CHMI model. While this investigation of the
462 delayed booster regimen was a serendipitous effect of the SARS-CoV-2 pandemic – not
463 unlike the original delayed fractional booster observations with RTS,S [6]– it now seems

464 likely that future clinical development of the PvDBP11 candidate will benefit from further
465 interrogation of delayed booster regimens. These findings are supported by data from an
466 independent RH5.1/Matrix-MTM clinical trial in malaria-exposed adults in Tanzania where
467 delayed booster dosing not only increases the frequency of circulating RH5-specific memory
468 B cells, but also RH5-specific plasma cells in the bone marrow.

469 Methods

470 Clinical trials

471 This study focused on the comparison of immune responses between groups vaccinated
472 with the *Plasmodium vivax* antigen DBPRII with different platforms and dosing regimens
473 (**Table 1** [11]). In brief, two Phase I/IIa vaccine efficacy trials (NCT04009096 and
474 NCT04201431) were conducted in parallel at a single site in the UK (Centre for Clinical
475 Vaccinology and Tropical Medicine, University of Oxford). NCT04009096 was an open label
476 trial to assess the ChAd63 and MVA viral-vectored vaccines encoding PvDBPII (VV-
477 PvDBPII), while the NCT04201431 trial assessed the protein vaccine PvDBPII in Matrix-M™
478 adjuvant from Novavax (PvDBPII/M-M). NCT04009096 viral vectors were administered at 0,
479 2 months (VV-M) or in a delayed dosing regimen (0, 17, 19 months; VV-D). For
480 NCT04201431, the protein/adjuvant was administered monthly (0, 1, 2 months; PA-M) or in
481 a delayed dosing regimen (0, 1, 14 months; PA-D). A subset of vaccinees from the
482 protein/adjuvant delayed dosing regimen returned for an additional booster at 19 months
483 (PA-DB). ChAd63-PvDBPII was administered at a dose of 5×10^{10} viral particles, MVA-
484 PvDBPII at 2×10^8 plaque forming units, and PvDBPII protein at 50µg mixed with 50µg
485 Matrix-M™. Delayed regimens were due to trial halts during the pandemic. Eligible
486 vaccinees were healthy, Duffy-positive, malaria-naïve adults, aged 18 to 45 years. Trials
487 were approved by the UK National Health Service Research Ethics Services (REC;
488 references 19/SC/0193 and 19/SC/0330) as well as by the UK Medicine and Healthcare
489 products Regulatory Agency (MHRA; reference CTA 21584/0414/001-0001 and CTA
490 21584/0418/001-0001). All vaccinees gave written informed consent.

491

492 This study also includes analyses of samples from a further Phase Ib clinical trial with
493 *Plasmodium falciparum* vaccine candidate RH5.1 (50µg) in Matrix-M™ adjuvant (50µg) in
494 malaria-endemic setting in Tanzania (NCT04318002). RH5.1/Matrix-M™ was administered
495 at either a monthly 0, 1, 2 months (M) or delayed 0, 1, 6 months (D) booster regimen. The

496 final vaccination in the delayed booster regimen was given at a fractionated RH5.1 antigen
497 dose of 10µg, rather than 50µg (the dose of Matrix-M™ was not fractionated and remained
498 50 µg). Eligible vaccinees were healthy adults (negative for malaria by blood smear at
499 screening), aged 18 to 45 years. The trial was approved by the Tanzanian Medicines and
500 Medical Devices Authority (reference TMDA0020/CTR/0006/01), the National Institute for
501 Medical Research (references NIMR/HQ/R.8a/Vol.IX/3537 and NIMR/HQ/R.8c/Vol.1/1887),
502 the Ifakara Health Institute Institutional Review Board (reference IHI/IRB/No:49-2020), and
503 the Oxford Tropical Research Ethics Committee (reference 9-20). All vaccinees gave written
504 informed consent.

505

506 [Methods details](#)

507 [Flow cytometry – B cells](#)

508 Cryopreserved PBMC from the DBPRII trial were thawed into R10 media (RPMI [R0883,
509 Sigma] supplemented with 10% heat-inactivated FCS [60923, Biosera], 100U/ml penicillin /
510 0.1mg/mL streptomycin [P0781, Sigma], 2mM L-glutamine [G7513, Sigma]) then washed
511 and rested in R10 for 1h. B cells were enriched (Human Pan-B cell Enrichment Kit [19554,
512 StemCell]) and then stained with viability dye FVS780 (565388, BD Biosciences). Next, B
513 cells were stained with anti-human CD19-BV786 (563325, BD Biosciences), anti-human
514 CD20-BUV395 (563782, BD Biosciences), anti-human IgG-BB515 (564581, BD
515 Biosciences), anti-human IgM-BV605 (562977, BD Biosciences), anti-human CD27-PE-Cy7
516 (560609, BD Biosciences), anti-human CD21-BV711 (563163, BD Biosciences), anti-human
517 CD38-BV480 (566137, BD Biosciences), anti-human CD138-APC-R700 (566050, BD
518 Biosciences), anti-human IgA-PerCP-Vio700 (130-113-478, Miltenyi) as well as two
519 fluorophore-conjugated DBPRII probes. Preparation of the DBPRII probes was based on our
520 previously published protocols with the *P. falciparum* blood-stage malaria antigen RH5 [12;
521 20]. In brief, monobiotinylated DBPRII was produced by transient co-transfection of
522 HEK293F cells with a plasmid encoding BirA biotin ligase and a plasmid encoding a

523 monoFC-fused, biotin acceptor peptide- and c-tagged full-length DBPRII. Monobiotinylated
524 DBPRII was purified by affinity chromatography (c-tag) and size exclusion chromatography.
525 The monoFC solubilisation domain was cleaved using TEV protease. Probes were freshly
526 prepared for each experiment, by incubation of monobiotinylated DBPRII with streptavidin-
527 PE (S866, Invitrogen) or streptavidin-APC (Biolegend, 17-4317-82) at an approximately 4:1
528 molar ratio to facilitate tetramer generation and subsequently centrifuging to remove
529 aggregates. Following surface staining, cells were permeabilised and fixed with Transcription
530 Factor Buffer Set (562574, BD Biosciences), stained with anti-human Ki67-BV650 (563757,
531 BD Biosciences), washed, and stored at 4°C until acquisition. Samples were acquired on a
532 Fortessa X20 flow cytometer with FACSDiva8.0 (both BD Biosciences). Samples were
533 analysed using FlowJo (v10; Treestar). Samples were excluded from analysis if <50 cells in
534 the parent population.

535

536 The B cell assay with cryopreserved samples from the RH5 clinical trial was performed as
537 above with two modifications to the protocol. First, RH5 probes rather than DBPRII probes
538 were used as previously described [12; 20]. Second, probe staining was repeated during the
539 intracellular cytokine staining step at a 1/10 dilution as compared to concentrations used for
540 surface staining.

541

542 See below for details of CITRUS analyses with B cell flow cytometry samples.

543

544 Flow cytometry – T cells

545 DBPRII peptide stimulation was used to detect DBPRII-specific T cells in an intracellular
546 cytokine staining (ICS) assay as previously described [11]. Cryopreserved PBMC were
547 thawed in R10 and rested before an 18h stimulation with medium alone, 2.5 µg/peptide/mL
548 of a PvDBPII 20mer peptide pool (Mimotopes; **Table 3**), or 1 µg/mL Staphylococcal
549 enterotoxin B (SEB; S-4881, Sigma; positive control). Anti-CD28 (1µg/ml; 16-0289-85,

550 eBioscience), anti-CD49d (1µg/ml; 16-0499-85, eBioscience) and anti-CD107a-PE-Cy5 (15-
551 1079-42, eBioscience) were included in the cell culture medium. Brefeldin A (00-4506-51,
552 eBioscience) and monensin (00-4505-51, eBioscience) were added after 2h. Following
553 incubation, PBMC were stained with viability dye Live/Dead Aqua (L34966, Invitrogen) and
554 anti-human CCR7-BV711 (353228, Biolegend). Cells were then permeabilised and fixed with
555 Cytotfix/Cytoperm (554714, BD Biosciences) before staining with anti-human CD14-eF450
556 (48-0149-42, eBioscience), anti-human CD19-eFl450 (48-0199-42, eBioscience), anti-
557 human CD8a-APC-eF780 (47-0088-42, eBioscience), anti-human IFN-γ-FITC (11-7319-82,
558 eBioscience), anti-human TNFα-PE-Cy7 (25-7349-8, eBioscience), anti-human CD3-AF700
559 (56-0038-82, eBioscience), anti-CD4-PerCP Cy5.5 (300530, Biolegend), anti-human IL-2-
560 BV650 (500334, Biolegend), anti-human IL5-PE (500904, Biolegend), anti-human IL13-APC
561 (501907 Biolegend), anti-human CD45RA-BV605 (304134, Biolegend). Finally, cells were
562 washed, and stored at 4°C until acquisition. Samples were acquired on a Fortessa X20 flow
563 cytometer with FACSDiva8.0 (both BD Biosciences). Samples were analysed using FlowJo
564 (v10; Treestar). Background cytokine responses to medium alone were subtracted from
565 DBPRII-specific responses. Samples were excluded from analysis if <50 cells in the parent
566 population.

567 **Table 3. Peptide pool for T cell stimulation.** The PvDBP II Sall amino acid sequence was
 568 used to design 20mer peptides overlapping by 12 amino acids and these were synthesized
 569 by Mimotopes, Australia. Each stock was reconstituted to 50mg/mL in DMSO. A
 570 200µg/peptide/mL working stock of PvDBP II peptides was prepared by adding an equal
 571 amount of each peptide to cell culture medium for a final total peptide concentration of
 572 8mg/mL.

Peptide Number	N-terminus	Amino Acid Sequence	C-terminus
1	H-	DHKKTISSAIINHAF LQNTVGSG(261)	-NH ₂
2	Biotin-	SGSGAIINHAF LQNTVMKNCNYKR	-NH ₂
3	Biotin-	SGSGQNTVMKNCNYKRKRERDWD	-NH ₂
4	Biotin-	SGSGNYKRKRERDWD CNTKKDVC	-NH ₂
5	Biotin-	SGSGRDWDCNTKKDVCIPDRRYQL	-NH ₂
6	Biotin-	SGSGKDVCIPDRRYQLCMKELTNL	-NH ₂
7	Biotin-	SGSGRYQLCMKELTNLVNNTDTNF	-NH ₂
8	Biotin-	SGSGLTNLVNNTDTNFHRDITFRK	-NH ₂
9	Biotin-	SGSGDTNFHRDITFRKLYLKRKLI	-NH ₂
10	Biotin-	SGSGTFRKLYLKRKLIYDAVEGD	-NH ₂
11	Biotin-	SGSGRKLIYDAVEGDLLLKLNNY	-NH ₂
12	Biotin-	SGSGVEGDLLLKLNNYRYNKDFCK	-NH ₂
13	Biotin-	SGSGLNNYRYNKDFCKDIRWSLGD	-NH ₂
14	Biotin-	SGSGDFCKDIRWSLGD FGDIIIMGT	-NH ₂
15	Biotin-	SGSGSLGDFGDIIIMGTMEGIGYS	-NH ₂
16	Biotin-	SGSGIMGTMEGIGYSKVVENNL R	-NH ₂
17	Biotin-	SGSGIGYSKVVENNLRSIFGTDEK	-NH ₂
18	Biotin-	SGSGNNLRSIFGTDEKAQQRKQW	-NH ₂
19	Biotin-	SGSGTDEKAQQRKQWWNESKAQI	-NH ₂
20	Biotin-	SGSGRKQWWNESKAQIWTAMMYSV	-NH ₂
21	Biotin-	SGSGKAQIWTAMMYSVKKRLKGNF	-NH ₂
22	Biotin-	SGSGMYSVKKRLKGNFIWICKLNV	-NH ₂
23	Biotin-	SGSGKGNFIWICKLNVAVNIEPQI	-NH ₂
24	Biotin-	SGSGKLNVAVNIEPQIYRWIREWG	-NH ₂
25	Biotin-	SGSGEPQIYRWIREWGRDYVSELP	-NH ₂
26	Biotin-	SGSGREWGRDYVSELPTEVQKLKE	-NH ₂
27	Biotin-	SGSGSELPTEVQKLKEKCDGKINY	-NH ₂
28	Biotin-	SGSGKLKEKCDGKINYTDKKVCKV	-NH ₂
29	Biotin-	SGSGKINYTDKKVCKVPPCQNACK	-NH ₂
30	Biotin-	SGSGVCKVPPCQNACKSYDQWITR	-NH ₂
31	Biotin-	SGSGNACKSYDQWITRKKNQWDVL	-NH ₂
32	Biotin-	SGSGWITRKKNQWDVLSNKFISVK	-NH ₂
33	Biotin-	SGSGWDVLSNKFISVKNAEKVQTA	-NH ₂
34	Biotin-	SGSGISVKNAEKVQTAGIVTPYDI	-NH ₂
35	Biotin-	SGSGVQTAGIVTPYDILKQELDEF	-NH ₂
36	Biotin-	SGSGPYDILKQELDEFNEVAFENE	-NH ₂
37	Biotin-	SGSGLDEFNEVAFENEINKRDGAY	-NH ₂
38	Biotin-	SGSGFENEINKRDGAYIELCVCSV	-NH ₂
39	Biotin-	SGSGDGAYIELCVCSVEEAKKNTQ	-NH ₂
40	Biotin-	SGSGIELCVCSVEEAKKNTQEVVT	-OH

573

574 ELISAs

575 For the DBPRII clinical trial, antigen-specific total IgG, IgG3, IgG4, IgA, IgA1 and IgM titres
576 were determined by standardised ELISA in accordance with published methodology [21].
577 Nunc MaxiSorp™ flat-bottom ELISA plates (44-2404-21, Invitrogen) were coated overnight
578 with 2µg/mL (for total IgG titres) or 5µg/mL (for IgG1, IgG3, IgG4, IgA, IgA1 and IgM titres) of
579 DBPRII Sall protein or 2µg/mL of sd3 protein in PBS. DBPRII protein was produced as
580 previously described [11], while sd3 protein was produced by transient transfection of
581 Expi395F cells with a plasmid encoding a monoFc, DBP Subdomain 3 (sequence as per
582 UniProt P22290 PVDR residues P387-S508) and a C-terminal c-tag. The monoFc was
583 cleaved using TEV protease and sd3 was purified by affinity chromatography (c-tag) and
584 size exclusion chromatography. Plates were washed with washing buffer composed of PBS
585 containing 0.05% TWEEN® 20 (P1379, Sigma-Aldrich) and blocked with 100µL of Starting
586 Block™ T20 (37538, ThermoFisher Scientific). After removing blocking buffer, standard
587 curve and internal controls were diluted in blocking buffer using a pool of high-titre vaccinee
588 plasma or serum, specific for each antigen and isotype or subclass being tested, and 50µL
589 of each dilution was added to the plate in duplicate. Test samples were diluted in blocking
590 buffer to a minimum dilution of 1:50 (or 1:100 for total IgG) and 50µL was added in triplicate.
591 Plates were incubated for 2 hours at 37°C (or 20°C for total IgG) and washed in washing
592 buffer. An alkaline phosphatase-conjugated secondary antibody was diluted at the
593 manufacturer's recommend minimum dilution for ELISA in blocking buffer. The antibody
594 used was dependent on the isotype or subclass being assayed and were as follows: IgG-AP
595 (A3187, Thermo Scientific), IgG1 Fc-AP (9054-04, Southern Biotech), IgG3 Hinge-AP (9210-
596 04, Southern Biotech), IgG4 Fc-AP (9200-04, Southern Biotech), IgA-AP (2050-04, Southern
597 Biotech), IgA1-AP (9130-04, Southern Biotech), and IgM-AP (2020-04, Southern Biotech).
598 50µL of the secondary antibody dilution was added to each well of the plate and incubated
599 for 1 h at 37°C (or 20°C for total IgG). Plates were developed using PNPP alkaline
600 phosphatase substrate (N2765, Sigma-Aldrich) for 1-4 h at 37°C (or approximately 15

601 minutes at 20°C for total IgG). Optical density at 405 nm was measured using an ELx808
602 absorbance reader (BioTek) until the internal control reached an OD₄₀₅ of 1. The reciprocal
603 of the internal control dilution giving an OD₄₀₅ of 1 was used to assign an AU value of the
604 standard. Gen5 ELISA software v3.04 (BioTek) was used to convert the OD₄₀₅ of test
605 samples into AU values by interpolating from the linear range of the standard curve fitted to
606 a four-parameter logistics model. Any samples with an OD₄₀₅ below the linear range of the
607 standard curve at the minimum dilution tested were assigned a minimum AU value according
608 to the lower limit of quantification of the assay. For assessment of IgG2 and IgA2 responses,
609 no anti-DBPRII IgG2 or IgA2 samples were available for standard curve generation.
610 Responses were measured on plates coated with 5 µg/mL DBPRII. Four wells were also
611 coated with RH5.1 protein for development control wells. Each sample was tested in
612 duplicate with six negative control serum samples and two development control serum
613 samples on the RH5.1 coated wells from a previous RH5.1/AS01 vaccine trial [4]. Secondary
614 antibodies used were IgG2 Fd-AP (9080-04) and IgA2-AP (9140-04). The assay was carried
615 out as above and plates were developed for 2-4 hours at 37°C.

616

617 For the RH5 clinical trial, serum antibody levels to full-length RH5 protein (RH5.1) were
618 assessed by standardised ELISA methodology as previously described [4; 22]. In brief, the
619 reciprocal of the test sample dilution giving an optical density of 1.0 at 405nm (OD_{405nm}) was
620 used to assign an ELISA unit value of the standard. The standard curve and Gen5 software
621 v3.04 (Agilent) was then used to convert the OD_{405nm} of test samples to arbitrary units (AU).
622 Responses are reported in µg/mL using conversion factor from AU generated by calibration-
623 free concentration analysis (CFCA) as previously reported [22].

624

625 Bone marrow aspirate processing and ELISPOTs

626 A single 10mL bone marrow aspirate was collected per vaccinee into EDTA in the RH5 trial.
627 Bone marrow mononuclear cells (BMMNC) were purified from aspirates by density

628 centrifugation on Lymphoprep (1114545, Axis Shield) following passage through a 70µm
629 nylon cell strainer (542070, Greiner Bio-One Ltd). BMMNC were cryopreserved for future
630 use in FCS (S1810, Biosera) with 10% DMSO (D2650, Sigma). Samples were subsequently
631 thawed and enriched for B cells using a Pan B Cell Enrichment Kit (19554, Stemcell) for
632 detection of RH5-specific plasma cells with an antibody-secreting cell (ASC) ELISPOT. In
633 brief, enriched bone marrow B cells were aliquoted onto MAIP ELISpot Plates (MAIPS4510,
634 Millipore) coated with 5µg/mL RH5 protein, PBS (negative control), or 50µg/mL polyvalent
635 goat anti-human immunoglobulin (positive control; H1700 Caltag). Plates were incubated for
636 16-18h at 37°C prior to cell removal and incubation with anti-human IgG conjugated to
637 alkaline phosphatase (γ-chain specific; 401442, Calbiochem). Finally, plates were developed
638 with BCIP/NBT (M0711A, Europa Bioproducts) and read on an AID ELISPOT Plate Reader
639 (AID). To note, for consistency all ASCs are referred to as plasma cells throughout this
640 report.

641

642 *In vivo* growth inhibition (IVGI)

643 *In vivo* growth inhibition (IVGI) has been reported elsewhere for the DBPRII trial [11]. In brief,
644 IVGI was calculated for each vaccinee as the percentage reduction in parasite multiplication
645 rate (PMR) relative to the mean PMR of the unvaccinated controls. PMR was modelled for
646 each vaccinee based on log₁₀ transformed qPCR data of the *P. vivax* 18S ribosomal RNA
647 gene, using a mean of three replicate qPCR results for each vaccinee per time point [11; 23;
648 24]. Further details of the IVGI/ PMR methodology in this trial can be found in the
649 Supplementary Appendix of the primary trial report [11].

650

651 Quantification and Statistical Analyses

652 Comparisons were performed between regimens with (two-tailed) Mann-Whitney tests or
653 Kruskal-Wallis test with Dunn's Correction for multiple comparisons (GraphPad Prism v9). A
654 *p* value of < 0.05 was considered statistically significant.

655

656 Specifics of the CITRUS analyses are outlined in further detail below. For all data, relevant
657 statistical tests and sample sizes are specified in figure legends.

658

659 Clustering of B cell flow cytometry data with CITRUS

660 Raw fcs files with file-internal compensation (i.e. acquisition-defined) from the B cell flow
661 cytometry assays with DBPR11 or RH5 trial samples were uploaded separately into
662 Cytobank. Live, single (B cell-enriched) lymphocytes were gated and then analysed with
663 CITRUS using equal event sampling. All fluorophore channels were used for clustering with
664 the exception of the probes and the viability stain. All groups and time points were run in a
665 single CITRUS analysis per trial. Median expression values for each fluorophore for each
666 CITRUS-defined cluster were exported per sample. Average expression values across all
667 samples for each fluorophore were then calculated per cluster to define FlowJo gating
668 strategies. Clusters with shared gating strategies were combined into new populations
669 (**Table 2**) for re-analysis in FlowJo. Ki67 was included in the CITRUS clustering but median
670 expression values did not facilitate defining a dichotomous gating strategy and thus Ki67
671 was not utilised in the population definitions. Samples were excluded from analysis if <50
672 cells in the parent population.

673 Acknowledgements

674 We thank the vaccinees and clinical staff for participating in and running the clinical trials
675 essential for this study, especially Fay Nugent, Jee-Sun Cho, Yrene Themistocleous,
676 Thomas Rawlinson, Alison Lawrie, Ian Poulton, Rachel Roberts, Iona Taylor, Sumi Biswas,
677 Julie Furze, Baktash Khozoe, Nicola Greenwood, Saumu Ahmed, Florence Milando, and
678 Neema Balige. We also thank Jenny Reimer and Cecilia Carnot at Novavax for providing the
679 Matrix-M™ adjuvant, Federica Cappuccini for guidance developing the T cell flow cytometry
680 assay, Robert Hedley and Vasiliki Tsioligka from the Sir William Dunn School of Pathology
681 Flow Cytometry Facility for assistance with sample acquisition and training, and the qPCR
682 team on the NCT04009096 and NCT04201431 trials (Duncan Bellamy, Hannah Davies,
683 Francesca Donnellan, Amy Flaxman, Reshma Kailath, Rebecca Makinson, Indra
684 Rudiansyah, and Marta Ulaszewska). CMN was supported by a Sir Henry Wellcome
685 Postdoctoral Fellowship (209200/Z/17/Z). SJD was supported by a Wellcome Trust Senior
686 Fellowship (106917/Z/15/Z) and is a Jenner Investigator. The NCT04009096 trial was
687 funded by the European Union’s Horizon 2020 research and innovation program under grant
688 agreement 733073 for MultiViVax. The NCT04201431 trial was funded by the Wellcome
689 Trust Malaria Infection Study in Thailand (MIST) program [212336/Z/18/Z]. The DBPRII
690 clinical trial was also supported in part by the UK Medical Research Council (MRC)
691 [G1100086] and the NIH Research (NIHR) Oxford Biomedical Research Center (BRC). The
692 views expressed are those of the author(s) and not necessarily those of the NHS, the NIHR
693 or the Department of Health. Development of PvDBPII as a vaccine candidate was
694 supported by grants from the Biotechnology Industry Research Assistance Council (BIRAC),
695 New Delhi and PATH Malaria Vaccine Initiative. MVDP was supported by grants from the Bill
696 and Melinda Gates Foundation and Department of Biotechnology (DBT), Government of
697 India. This work was also supported in part by grants from Agence Nationale de Recherche
698 to CEC (ANR-18-CE15-0026 and ANR 21 CE15-0013-01). CEC is supported by the French
699 Government’s Laboratoire d’Excellence “PARAFRAP” (ANR-11-LABX-0024-PARAFRAP).

700 The NCT04318002 trial was funded by the EDCTP2 programme supported by the European
701 Union (grant number RIA2016V-1649-MMVC). The views and opinions of authors expressed
702 herein do not necessarily state or reflect those of EDCTP. In both NCT04201431 and
703 NCT04318002 trials the Matrix-M™ adjuvant was provided by Novavax.

704

705 [Author contributions](#)

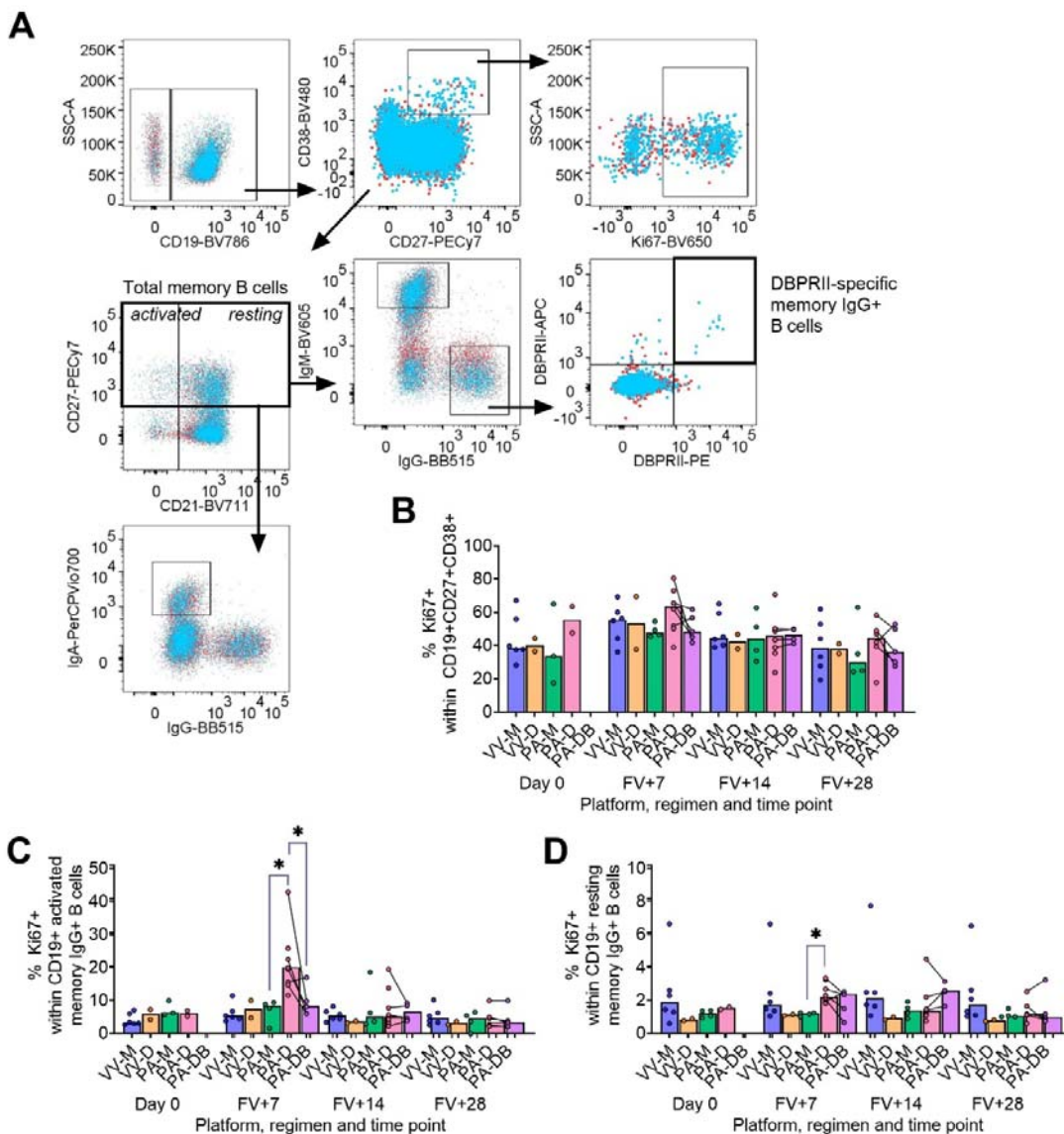
706 CMN led the study. AIO, AMM and SJD were chief, principal or lead investigators on the
707 clinical trials. JRB, SES, CGM, KMM, MMH, AML, WFK, IMM, KM, MB, HD, LK, NE, SR,
708 CMN performed experiments and/or oversaw critical sample processing. JRB, SES, NE and
709 CMN analysed and/or reviewed data. VSC, PM and CEC contributed the PvDBPII vaccine.
710 JRB and CMN wrote the manuscript.

711

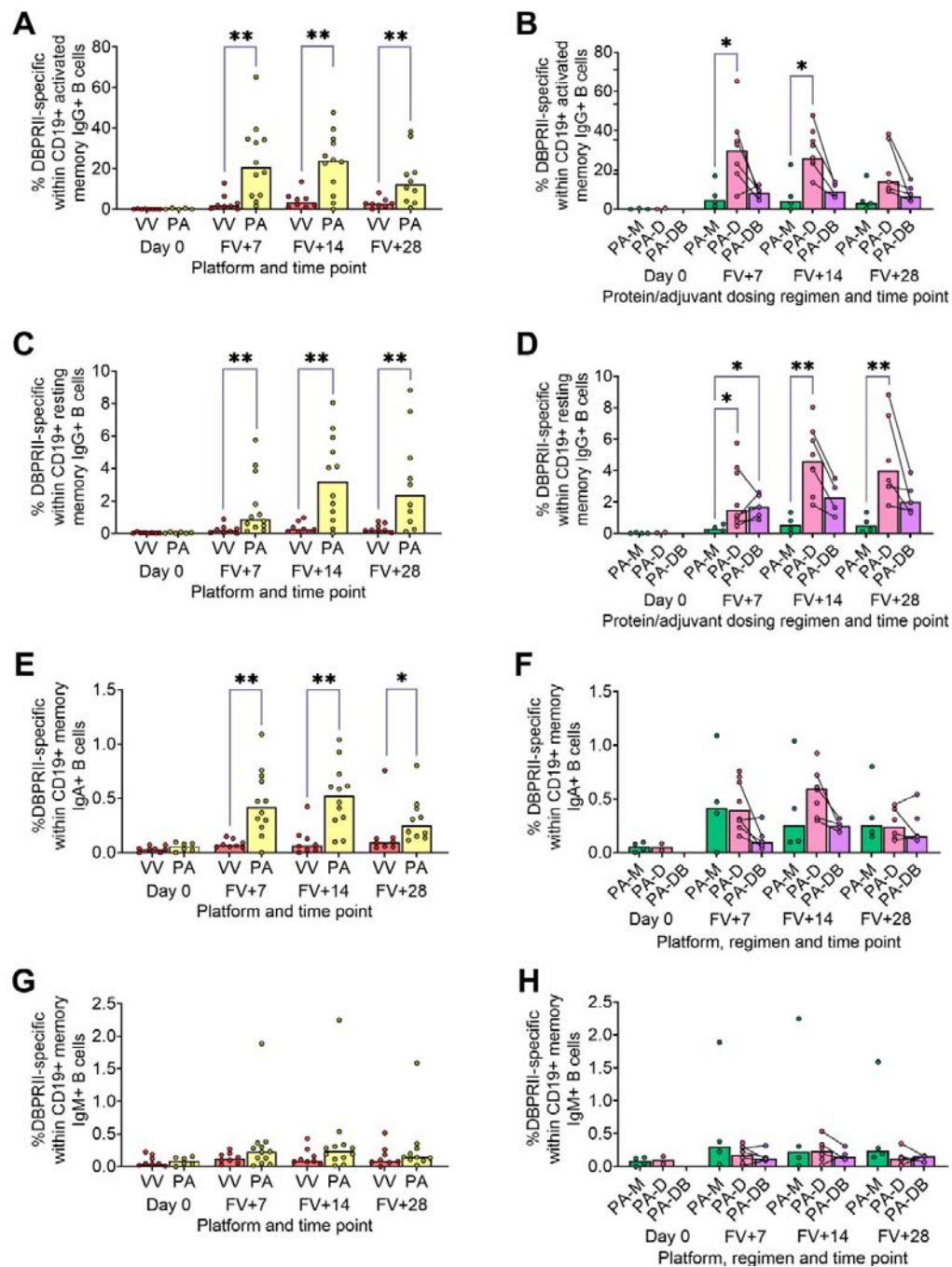
712 [Declaration of interests](#)

713 SJD is a named inventor on patent applications relating to RH5 malaria vaccines and
714 adenovirus-based vaccines, and is an inventor on intellectual property licensed by Oxford
715 University Innovation to AstraZeneca. AMM has an immediate family member who is an
716 inventor on patent applications relating to RH5 malaria vaccines and adenovirus-based
717 vaccines, and is an inventor on intellectual property licensed by Oxford University Innovation
718 to AstraZeneca. CEC is an inventor on patents that relate to binding domains of erythrocyte-
719 binding proteins of *Plasmodium* parasites including *P. vivax* DBP.

720 Supplemental Figures



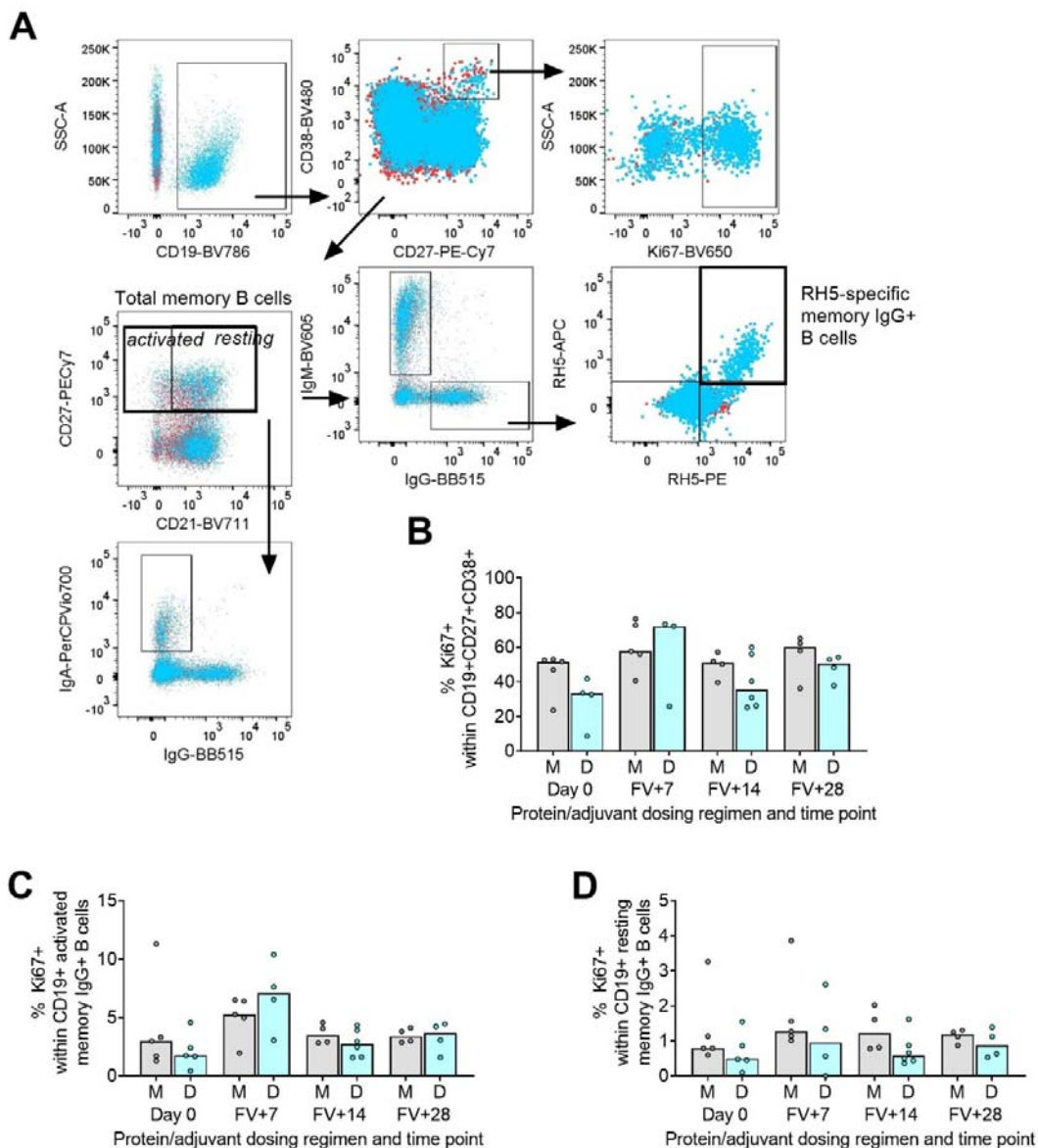
722
 723 Supplemental Figure 1. DBPRII B cell gating strategy and expression of proliferation marker Ki67.
 724 PBMC from pre-vaccination (Day 0) and post-final vaccination (FV) time points were analysed for B cell
 725 responses by flow cytometry. (A) Gating strategy shows identification of CD19+ B cells within live single (B cell-
 726 enriched) lymphocytes, and definition of CD38+CD27+ plasma cells within this population. Total memory cells
 727 are defined as CD27+ non-plasma cells (following use of a NOT gate to exclude plasma cells; indicated with thick
 728 black box); activated and resting memory B cells are more specifically categorised as CD21-CD27+ or
 729 CD21+CD27+, respectively. IgG+, IgM+ or IgA+ populations are subsequently gated within total memory cells.
 730 Proliferating (Ki67+) or vaccine-specific (those co-staining with DBPRII-PE and DBPRII-APC probes as indicated
 731 by thick black box) cells are defined within the plasma cell or isotype-specific memory B cell populations.
 732 Example shows Ki67 expression of plasma cells and DBPRII-specific gating on memory IgG+ B cells. A FV+14
 733 sample (blue) is overlaid on a matched Day 0 sample (red) for all plots. Frequencies of Ki67+ cells shown within
 734 plasma cells (B), activated IgG+ memory B cells (C), and resting IgG+ memory B cells (D). VV-M = ChAd63-MVA
 735 viral vector monthly dosing; VV-D ChAd63-MVA delayed booster dosing; PA-M = protein/adjuvant monthly
 736 dosing; PA-D = protein/adjuvant delayed booster dosing; PA-DB = protein/adjuvant delayed booster dosing with
 737 extra booster. Post-vaccination comparisons were performed between protein/adjuvant dosing regimens by
 738 Kruskal Wallis test with Dunn's correction for multiple comparisons. Sample sizes for all assays were based on
 739 sample availability; each circle represents a single sample. VV-M/VV-D/PA-M/PA-D/PA-DB: Day 0 = 6/2/3-4/2/na,
 740 FV+7 = 6/2/4/8/5, FV+14 = 6/2/4/8/4, FV+28 = 6/2/4/6/5. PA-D vaccinees returning in the PA-DB group are
 741 connected by lines. Bars represent medians. * $p < 0.05$.



742
743
744
745
746
747
748
749
750
751
752
753
754
755
756
757
758

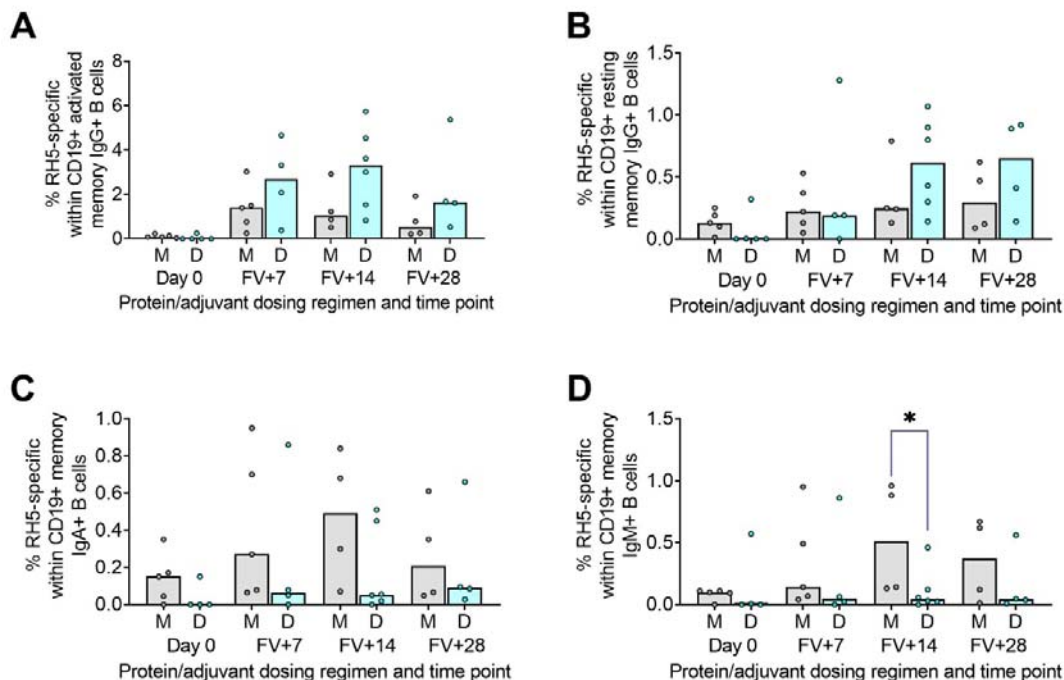
Supplemental Figure 2. Extended DBPRII-specific memory B cell responses.

PBMC from pre-vaccination (Day 0) and post-final vaccination (FV) time points were analysed for B cell responses by flow cytometry; gating strategies are as described in Methods and **Supplemental Figure 1**. Frequencies of DBPRII-specific B cells – identified by probe staining – were compared within activated memory IgG+ B cells (**A-B**), resting memory IgG+ B cells (**C-D**), total memory IgA+ B cells (**E-F**), and total memory IgM+ B cells (**G-H**) between vaccine platforms (**A, C, E, G**) or protein/adjuvant dosing regimens (**B, D, F, H**). VV = ChAd63-MVA viral vectors; PA = PvDBPII protein/adjuvant [PA-M and PA-D]; PA-M = PvDBPII protein/adjuvant monthly dosing; PA-D = PvDBPII protein/adjuvant delayed booster dosing; PA-DB = PvDBPII protein/adjuvant delayed booster dosing with extra booster. Post-vaccination comparisons were performed between DBPRII platforms (**A, C, E, G**) with Mann-Whitney U tests, or between PvDBPII protein/adjuvant dosing regimens by Kruskal Wallis test with Dunn's correction for multiple comparisons (**B, D, F, H**). Sample sizes for all assays were based on sample availability; each circle represents a single sample. (**A, C, E, G**) VV/PA: Day 0 = 8/5-6, FV+7 = 8/12, FV+14 = 8/12, FV+28 = 8/10. (**B, D, F, H**) PA-M/PA-D/PA-DB: Day 0 = 3-4/2/na, FV+7 = 4/8/5, FV+14 = 4/8/4, FV+28 = 4/6/5. (**E-F**) M/D: Day 0 = 5/1-4, FV+7 = 4-5/3-4, FV+14 = 4/6, FV+28 = 4/4. PA-D vaccinees returning in the PA-DB group are connected by lines. Bars represent medians. * $p < 0.05$, ** $p < 0.01$.



759
760
761
762
763
764
765
766
767
768
769
770
771
772
773
774
775

Supplemental Figure 3. RH5 B cell gating strategy and expression of proliferation marker Ki67. PBMC from pre-vaccination (Day 0) and post-final vaccination (FV) time points were analysed for B cell responses by flow cytometry. (A) Gating strategy shows identification of CD19+ B cells within live single (B cell-enriched) lymphocytes, and definition of CD38+CD27+ plasma cells within this population. Total memory cells are defined as CD27+ non-plasma cells (using a NOT gate to exclude plasma cells; indicated with thick black box); activated and resting memory B cells are more specifically categorised as CD21-CD27+ or CD21+CD27+, respectively. IgG+, IgM+ or IgA+ populations are subsequently gated within total memory cells. Proliferating (Ki67+) or vaccine-specific (those co-staining with RH5-PE and RH5-APC probes as indicated by thick black box) cells are defined within the plasma cell or isotype-specific memory B cell populations. Example shows Ki67 expression of plasma cells and RH5-specific gating on memory IgG+ B cells. A FV+14 sample (blue) is overlaid on a matched Day 0 sample (red) for all plots. Frequencies of Ki67+ cells shown within plasma cells (B), activated IgG+ memory B cells (C), and resting IgG+ memory B cells (D). M = RH5.1/adjutant monthly dosing; D = RH5.1/adjutant delayed booster dosing. Post-vaccination comparisons were performed between dosing regimens with Mann-Whitney U tests. Sample sizes for all assays were based on sample availability; each circle represents a single sample. (B-D) VV/PA: Day 0 = 5/4-5, FV+7 = 5/3-4, FV+14 = 4/6, FV+28 = 4/4. Bars represent medians.



776

777

Supplemental Figure 4. Extended RH5-specific memory B cell responses.

778

PBMC from pre-vaccination (Day 0) and post-final vaccination (FV) time points were analysed for B cell

779

responses by flow cytometry; gating strategies are as described in Methods and **Supplemental Figure 3**.

780

Frequencies of RH5-specific B cells – identified by probe staining – were compared within activated memory

781

IgG+ B cells (**A**), resting memory IgG+ B cells (**B**), total memory IgA+ B cells (**C**), and total memory IgM+ B cells

782

(**D**) between dosing regimens. M = RH5.1/adjutant monthly dosing; D = RH5.1/adjutant delayed booster dosing.

783

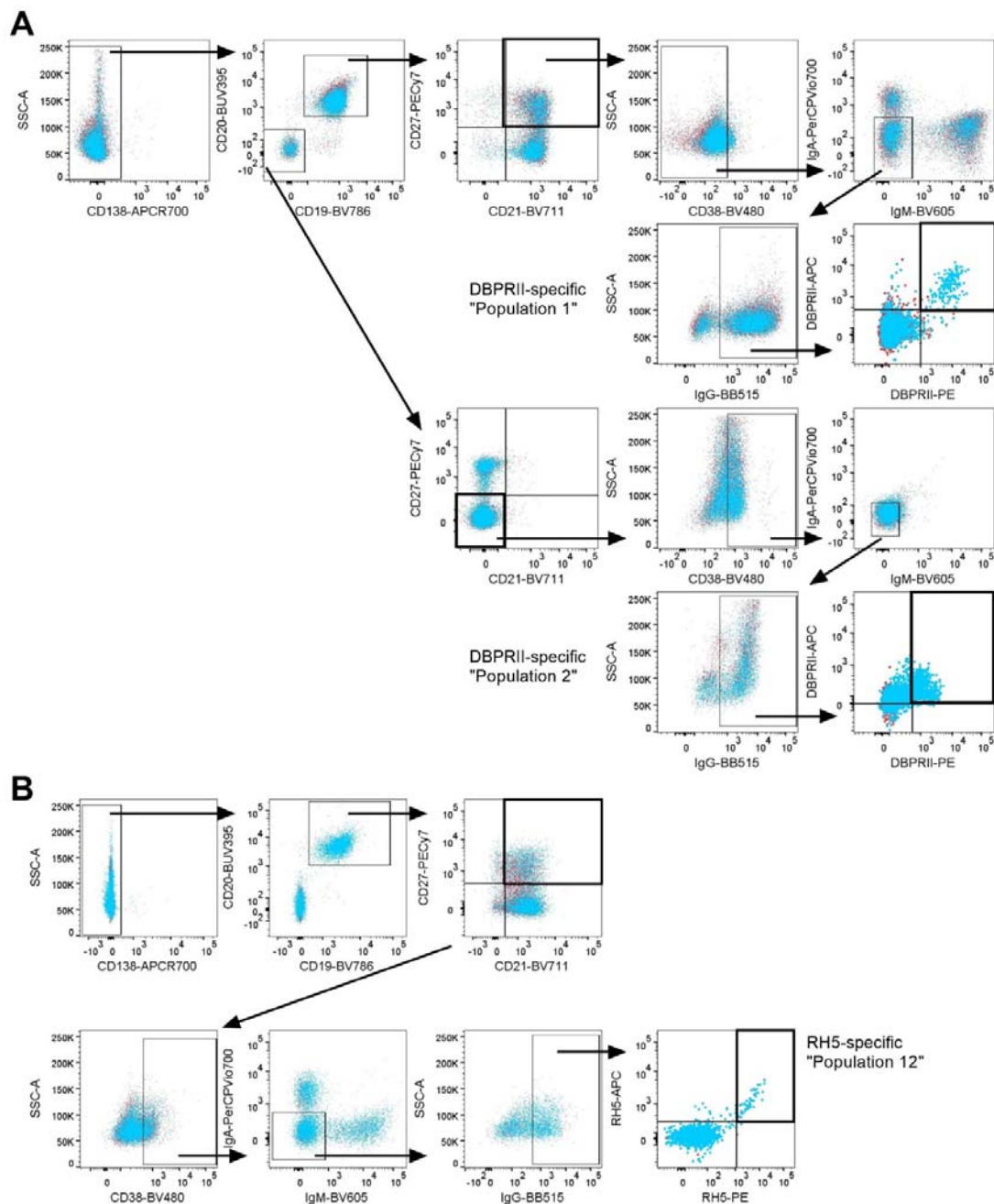
Post-vaccination comparisons were performed between dosing regimens with Mann-Whitney U tests. Sample

784

sizes for all assays were based on sample availability; each circle represents a single sample. (**B-D**) VV/PA: Day

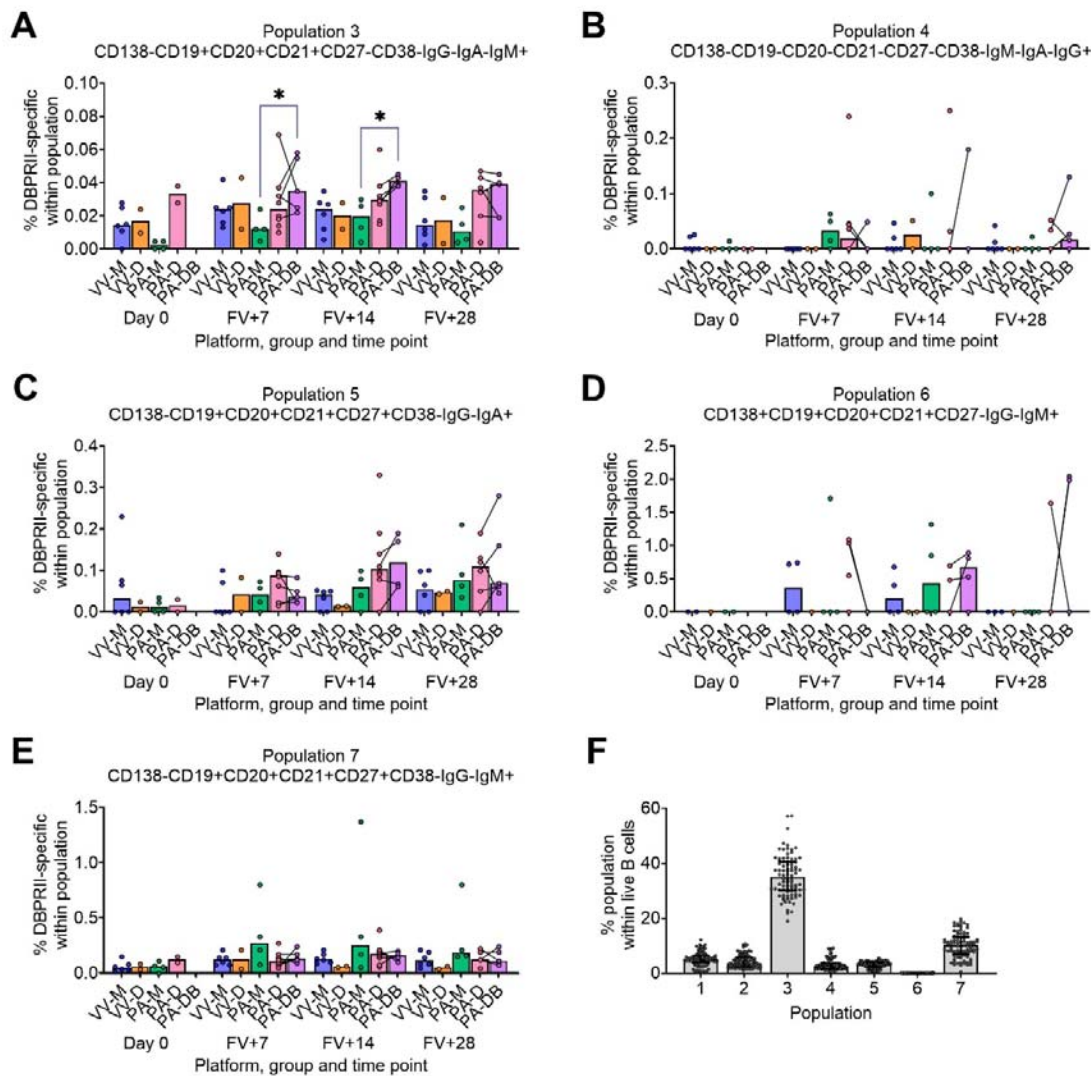
785

0 = 5/4-5, FV+7 = 5/4 FV+14 = 4/6, FV+28 = 4/4. Bars represent medians. * $p < 0.05$.



786
787
788
789
790
791
792
793
794
795
796

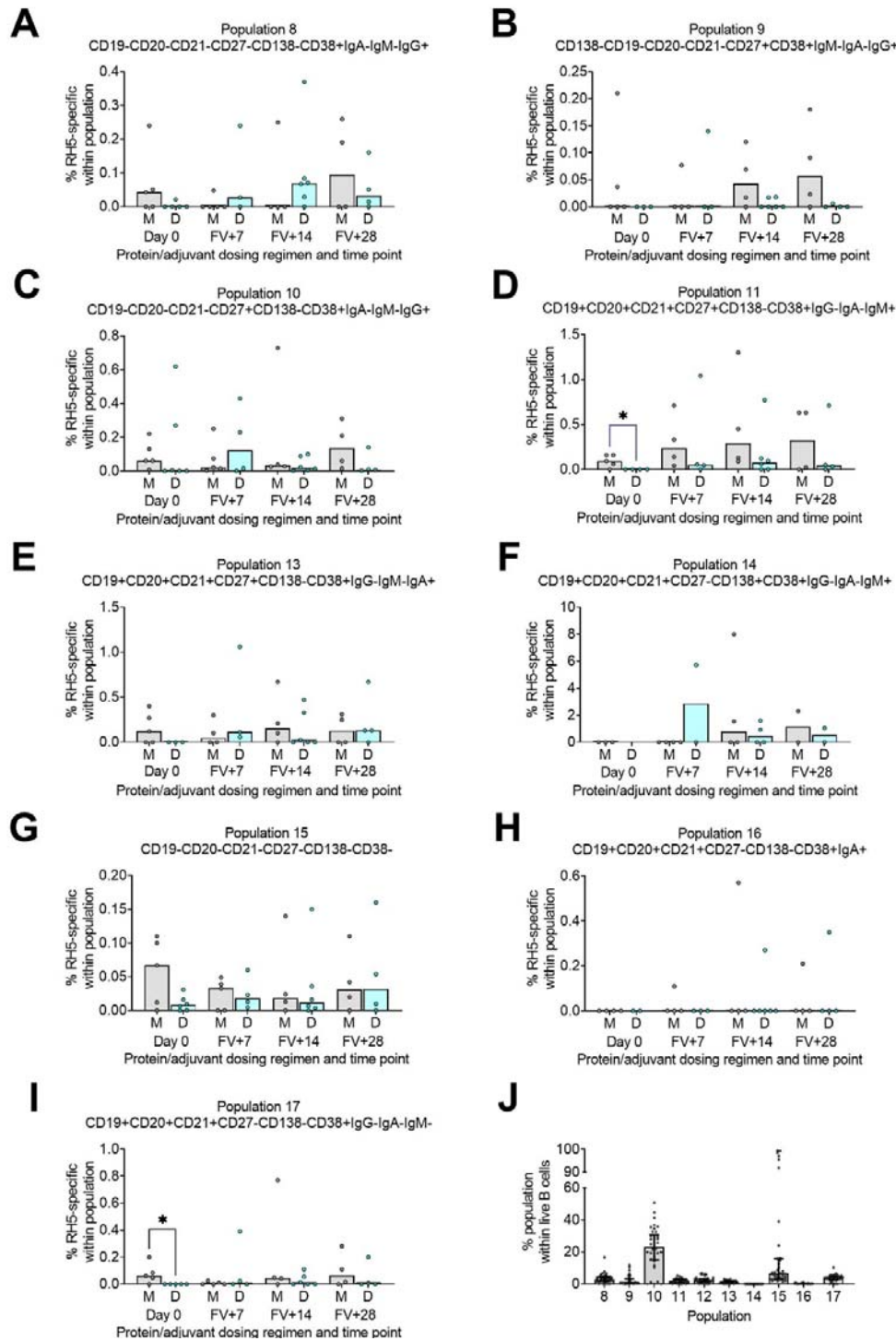
Supplemental Figure 5. Gating strategies for key agnostically-defined B cell populations via CITRUS. CITRUS was run on single live (B cell-enriched) lymphocyte flow cytometry fcs files to agnostically define the main B cell populations within either DBPR11 or RH5 trial samples. Median marker expression within each cluster was used to define gating strategies for B cell populations in FlowJo, which were re-analysed for DBPR11- or RH5-specific responses through probe staining. (A) Gating strategy shows identification of "Population 1" (CD19+CD20+CD21+CD27+CD138-CD38-IgM-IgA-IgG+) and "Population 2" (CD19-CD20-CD21-CD27-CD138-CD38-IgM-IgA-IgG+) within the DBPR11 trial and DBPR11-specific cells within these populations. (B) Gating strategy shows identification of "Population 12" (CD19+CD20+CD21+CD27+CD138-CD38-IgM-IgA-IgG+) within the RH5 trial. A FV+14 sample (blue) is overlaid on a matched Day 0 sample (red) for all plots. See **Table 2** for a full list of populations defined via CITRUS.



797
798
799
800
801
802
803
804
805
806
807
808
809
810
811
812

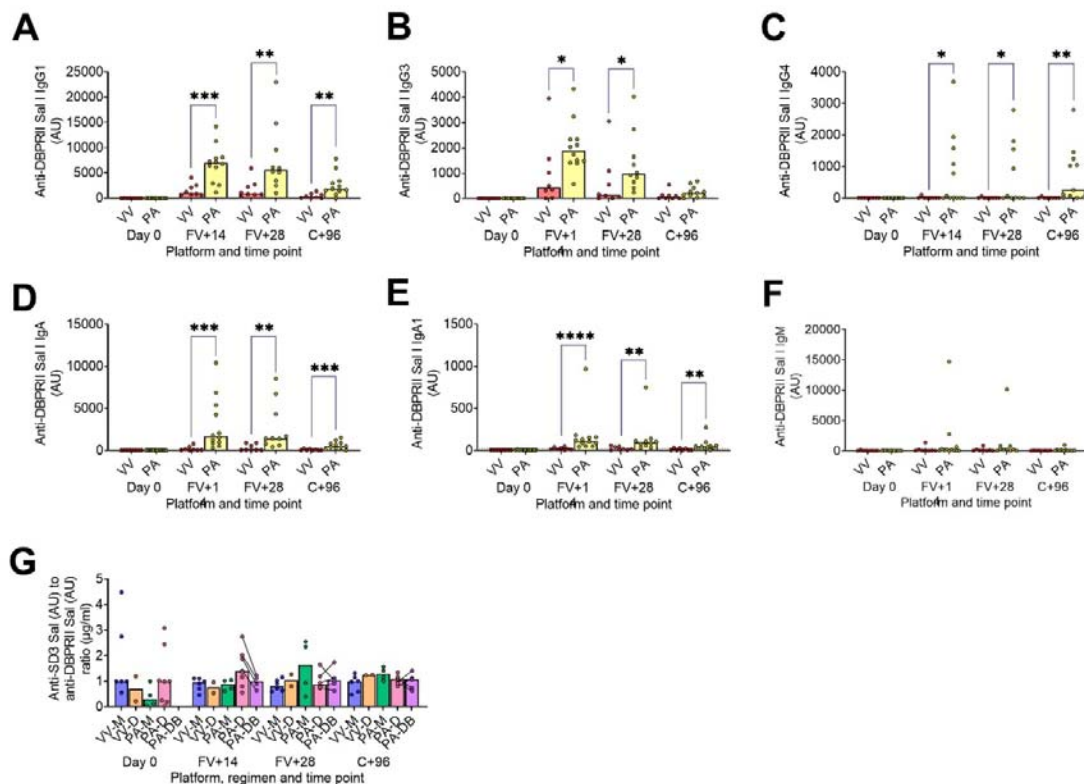
Supplemental Figure 6. DBPRII-specific responses within agnostically-defined B cell populations.

CITRUS was run on single live (B cell-enriched) lymphocyte flow cytometry fcs files to agnostically define the main B cell populations within DBPRII trial samples. Median marker expression within each cluster was used to define gating strategies for B cell populations in FlowJo, which were re-analysed for DBPRII-specific responses through probe staining (A-E). Population definitions are annotated on individual figures. (F) Frequencies of each population within single live B cells (enriched from lymphocytes; see also Table 2) of all samples. VV-M = ChAd63-MVA viral vector monthly dosing; VV-D ChAd63-MVA delayed booster dosing; PA-M = PvDBPII protein/adjuvant monthly dosing; PA-D = PvDBPII protein/adjuvant delayed booster dosing; PA-DB = PvDBPII protein/adjuvant delayed booster dosing with extra booster. FV = final vaccination. Post-vaccination comparisons were performed between PvDBPII protein/adjuvant dosing regimens by Kruskal Wallis test with Dunn's correction for multiple comparisons (A-E). Sample sizes for all assays were based on sample availability; each circle represents a single sample. (A-C, E) VV-M/VV-D/PA-M/PA-D/PA-DB: Day 0 = 6/2/4/2/na, FV+7 = 6/2/4/8/5, FV+14 = 6/2/4/8/4, FV+28 = 6/2/4/6/5. PA-D vaccinees returning in the PA-DB group are connected by lines. (D) VV-M/VV-D/PA-M/PA-D/PA-DB: Day 0 = 2/1/2/0/na, FV+7 = 4/1/4/8/4, FV+14 = 4/2/4/8/4, FV+28 = 3/1/4/5/5. (F) $n = 86$ for all populations. Bars represent medians. * $p < 0.05$.



Supplemental Figure 7. RH5-specific responses within agnostically-defined B cell populations.

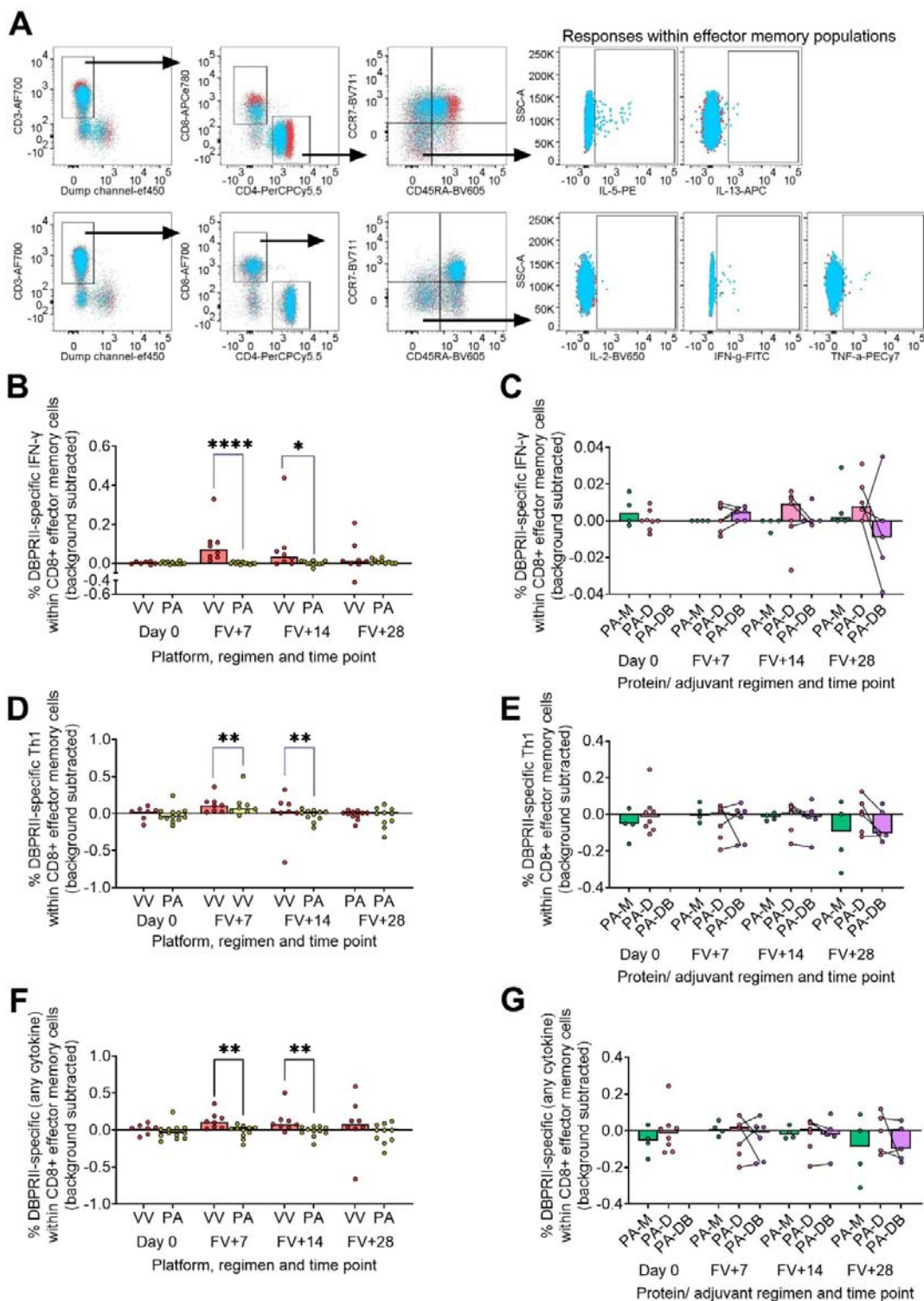
CITRUS was run on single live (B cell-enriched) lymphocyte flow cytometry fcs files to agnostically define the main B cell populations within RH5 trial samples. Median marker expression within each cluster was used to define gating strategies for B cell populations in FlowJo, which were re-analysed for RH5-specific responses through probe staining (A-I). Population definitions are annotated on individual figures. (J) Frequencies of each population within single live B cells (enriched from lymphocytes; see also **Table 2**) of all samples. M = RH5.1/adjuvant monthly dosing; D = RH5.1/adjuvant delayed booster dosing. FV = final vaccination. Post-vaccination comparisons were performed between dosing regimens with Mann-Whitney U tests (A-I). Sample sizes for all assays were based on sample availability; each circle represents a single sample. (A-G, I) M/D Day 0 = 4-5/2-6, FV+7 = 4-5/3-4, FV+14 = 4/6, FV+28 = 4/4. (H) M/D Day 0 = 3/0, FV+7 = 4/2, FV+14 = 4/4, FV+28 = 2/2. (J) $n = 38$ for all populations. Bars represent medians. * $p < 0.05$.



826
827
828
829
830
831
832
833
834
835
836
837
838
839
840
841
842

Supplemental Figure 8. DBPRII-specific peak antibody responses and serum maintenance.

Standardised ELISAs were developed to report anti-DBPRII specific or anti-subdomain 3 (sd3) antibody responses in pre-vaccination (Day 0) and post-final vaccination (FV) serum samples. Responses were compared between vaccine platforms for IgG1 (A), IgG3 (B), IgG4 (C), IgA (D), IgA1 (E), and IgM (F). IgG2 and IgA2 responses were below the limit of detection (not shown). The ratio of anti-sd3 to anti-DBPRII was also calculated for total IgG (G). VV = ChAd63-MVA viral vectors; PA = PvDBP11 protein/adjuvant [PA-M and PA-D]; VV-M = ChAd63-MVA viral vector monthly dosing; VV-D ChAd63-MVA delayed booster dosing; PA-M = protein/adjuvant monthly dosing; PA-D = protein/adjuvant delayed booster dosing; PA-DB = protein/adjuvant delayed booster dosing with extra booster. C+96 = 96 days after controlled human malaria infection (approximately 16-weeks after FV). Post-vaccination comparisons were performed between platforms (A-F) with Mann-Whitney U tests, or between protein/adjuvant dosing regimens by Kruskal Wallis test with Dunn's correction for multiple comparisons (G). Sample sizes for all assays were based on sample availability; each circle represents a single sample. (A-F) VV/PA: Day 0 = 8/12, FV+14 = 8/12, FV+28 = 8/10. (G) VV-M/VV-D/PA-M/PA-D/PA-DB: Day 0 = 6/2/4/8/na, FV+14 = 6/2/4/8/4, FV+28 = 6/2/4/6/5, C+96 = 6/2/4/7/5. PA-D vaccinees returning in the PA-DB group are connected by lines. Bars represent medians. * $p < 0.05$, ** $p < 0.01$, *** $p < 0.001$, **** $p < 0.0001$.



843
844

845 Supplemental Figure 9. DBPRII-specific T cell gating strategy and CD8+ effector memory responses.
846 PBMC from pre-vaccination (Day 0) and post-final vaccination (FV) time points were analysed for T cell
847 responses by intracellular cytokine staining. (A) Gating strategy shows identification of live T cells within single
848 lymphocytes [dump channel includes viability stain, anti-CD14, and anti-CD19; see Methods], and definition of
849 CD4+ and CD8+ T cells within this population. Effector memory CD4+ or CD8+ T cells are identified as CD45RA-
850 CCR7-. Finally, DBPRII-specific T cell responses are defined through detection of intracellular Th2 cytokines (top

851 row; IL-5, IL-13;) or Th1 cytokines (bottom row; IL-2, IFN- γ , TNF- α) following DBPRII peptide pool stimulation. A
852 FV+7 sample (blue) is overlaid on a matched Day 0 sample (red) for all plots (CD4+ effector memory from
853 protein/adjuvant vaccinee used as top row Th2 example; CD8+ effector memory from viral vector vaccinee used
854 as bottom row Th1 example).
855 DBPRII-specific effector memory CD4+ or CD8+ T cells are reported as frequencies producing cytokines in
856 response to peptide stimulation after background subtraction of cytokine-positive cells in matched samples
857 cultured with media alone. Using an 'OR' gate, responses were reported for all cytokines (cells producing any of
858 IL-5, IL-13, IL-2, IFN- γ , or TNF- α), Th1 cytokines (IL-2, IFN- γ or TNF- α only), or Th2 cytokine (IL-5 or IL-13 only;
859 see **Figure 4**). CD8+ effector memory T cells IFN- γ (**B-C**), Th1 (**D-E**) or any cytokine (**F-G**) responses were
860 compared between vaccine platforms (**B, D, F**) or protein/adjuvant dosing regimens (**C, E, G**). VV = ChAd63-
861 MVA viral vectors; PA = PvDBPII protein/adjuvant [PA-M and PA-D]; PA-M = PvDBPII protein/adjuvant monthly
862 dosing; PA-D = PvDBPII protein/adjuvant delayed booster dosing; PA-DB = PvDBPII protein/adjuvant delayed
863 booster dosing with extra booster. Post-vaccination comparisons were performed between DBPRII platforms by
864 Mann Whitney U test (**B, D, F**), or protein/adjuvant dosing regimens by Kruskal Wallis test with Dunn's correction
865 for multiple comparisons (**C, E, G**). Sample sizes for all assays were based on sample availability; each circle
866 represents a single sample. (**B, D, F**) VV/PA: Day 0 = 7/12, FV+7 = 8/11, FV+14 = 8/11, FV+28 = 8/10. (**C, E, G**)
867 PA-M/PA-D/PA-DB: Day 0 = 4/8/na, FV+7 = 4/7/6, FV+14 = 4/7/5, FV+28 = 4/6/5. PA-D vaccinees returning in
868 the PA-DB group are connected by lines. Bars represent medians. * $p < 0.05$, ** $p < 0.01$, **** $p < 0.0001$.

869 References

- 870 [1] A. Flaxman, N.G. Marchevsky, D. Jenkin, J. Aboagye, P.K. Aley, B. Angus, S. Belij-
871 Rammerstorfer, S. Bibi, M. Bittaye, F. Cappuccini, P. Cicconi, E.A. Clutterbuck, S.
872 Davies, W. Dejnirattisai, C. Dold, K.J. Ewer, P.M. Folegatti, J. Fowler, A.V.S. Hill, S.
873 Kerridge, A.M. Minassian, J. Mongkolsapaya, Y.F. Mujadidi, E. Plested, M.N.
874 Ramasamy, H. Robinson, H. Sanders, E. Sheehan, H. Smith, M.D. Snape, R. Song,
875 D. Woods, G. Sreaton, S.C. Gilbert, M. Voysey, A.J. Pollard, T. Lambe, and
876 C.V.T.g. Oxford, Reactogenicity and immunogenicity after a late second dose or a
877 third dose of ChAdOx1 nCoV-19 in the UK: a substudy of two randomised controlled
878 trials (COV001 and COV002). *Lancet* 398 (2021) 981-990.
- 879 [2] M. Voysey, S.A. Costa Clemens, S.A. Madhi, L.Y. Weckx, P.M. Folegatti, P.K. Aley, B.
880 Angus, V.L. Baillie, S.L. Barnabas, Q.E. Bhorat, S. Bibi, C. Briner, P. Cicconi, E.A.
881 Clutterbuck, A.M. Collins, C.L. Cutland, T.C. Darton, K. Dheda, C. Dold, C.J.A.
882 Duncan, K.R.W. Emary, K.J. Ewer, A. Flaxman, L. Fairlie, S.N. Faust, S. Feng, D.M.
883 Ferreira, A. Finn, E. Galiza, A.L. Goodman, C.M. Green, C.A. Green, M. Greenland,
884 C. Hill, H.C. Hill, I. Hirsch, A. Izu, D. Jenkin, C.C.D. Joe, S. Kerridge, A. Koen, G.
885 Kwatra, R. Lazarus, V. Libri, P.J. Lillie, N.G. Marchevsky, R.P. Marshall, A.V.A.
886 Mendes, E.P. Milan, A.M. Minassian, A. McGregor, Y.F. Mujadidi, A. Nana, S.D.
887 Padayachee, D.J. Phillips, A. Pittella, E. Plested, K.M. Pollock, M.N. Ramasamy, A.J.
888 Ritchie, H. Robinson, A.V. Schwarzbold, A. Smith, R. Song, M.D. Snape, E. Sprinz,
889 R.K. Sutherland, E.C. Thomson, M.E. Torok, M. Toshner, D.P.J. Turner, J.
890 Vekemans, T.L. Villafana, T. White, C.J. Williams, A.D. Douglas, A.V.S. Hill, T.
891 Lambe, S.C. Gilbert, A.J. Pollard, and C.V.T.G. Oxford, Single-dose administration
892 and the influence of the timing of the booster dose on immunogenicity and efficacy of
893 ChAdOx1 nCoV-19 (AZD1222) vaccine: a pooled analysis of four randomised trials.
894 *Lancet* 397 (2021) 881-891.
- 895 [3] R.P. Payne, S. Longet, J.A. Austin, D.T. Skelly, W. Dejnirattisai, S. Adele, N. Meardon, S.
896 Faustini, S. Al-Taei, S.C. Moore, T. Tipton, L.M. Hering, A. Angyal, R. Brown, A.R.
897 Nicols, N. Gillson, S.L. Dobson, A. Amini, P. Supasa, A. Cross, A. Bridges-Webb,
898 L.S. Reyes, A. Linder, G. Sandhar, J.A. Kilby, J.K. Tyerman, T. Altmann, H. Hornsby,
899 R. Whitham, E. Phillips, T. Malone, A. Hargreaves, A. Shields, A. Saei, S. Foulkes, L.
900 Stafford, S. Johnson, D.G. Wootton, C.P. Conlon, K. Jeffery, P.C. Matthews, J.
901 Frater, A.S. Deeks, A.J. Pollard, A. Brown, S.L. Rowland-Jones, J. Mongkolsapaya,
902 E. Barnes, S. Hopkins, V. Hall, C. Dold, C.J.A. Duncan, A. Richter, M. Carroll, G.
903 Sreaton, T.I. de Silva, L. Turtle, P. Klenerman, S. Dunachie, and P. Consortium,
904 Immunogenicity of standard and extended dosing intervals of BNT162b2 mRNA
905 vaccine. *Cell* (2021).
- 906 [4] A.M. Minassian, S.E. Silk, J.R. Barrett, C.M. Nielsen, K. Miura, A. Diouf, C. Loos, J.K.
907 Fallon, A.R. Michell, M.T. White, N.J. Edwards, I.D. Poulton, C.H. Mitton, R.O.
908 Payne, M. Marks, H. Maxwell-Scott, A. Querol-Rubiera, K. Bisnauthsing, R. Batra, T.
909 Ogrina, N.J. Brendish, Y. Themistocleous, T.A. Rawlinson, K.J. Ellis, D. Quinkert, M.
910 Baker, R. Lopez Ramon, F. Ramos Lopez, L. Barfod, P.M. Folegatti, D. Silman, M.
911 Dattoo, I.J. Taylor, J. Jin, D. Pulido, A.D. Douglas, W.A. de Jongh, R. Smith, E.
912 Berrie, A.R. Noe, C.L. Diggs, L.A. Soisson, R. Ashfield, S.N. Faust, A.L. Goodman,
913 A.M. Lawrie, F.L. Nugent, G. Alter, C.A. Long, and S.J. Draper, Reduced blood-stage
914 malaria growth and immune correlates in humans following RH5 vaccination. *Med (N*
915 *Y)* 2 (2021) 701-719 e19.
- 916 [5] C.M. Nielsen, J.R. Barrett, C. Davis, J.K. Fallon, C. Goh, A.R. Michell, C. Griffin, A. Kwok,
917 C. Loos, S. Darko, F. Laboune, M. Tekman, A. Diouf, K. Miura, J.R. Francica, A.
918 Ransier, C.A. Long, S.E. Silk, R.O. Payne, A.M. Minassian, D.A. Lauffenburger, R.A.
919 Seder, D.C. Douek, G. Alter, and S.J. Draper, Delayed boosting improves human
920 antigen-specific Ig and B cell responses to the RH5.1/AS01B malaria vaccine. *JCI*
921 *Insight* 8 (2023).

- 922 [6] J.A. Stoute, M. Slaoui, D.G. Heppner, P. Momin, K.E. Kester, P. Desmons, B.T. Wellde,
923 N. Garcon, U. Krzych, M. Marchand, W.R. Ballou, and J.D. Cohen, A preliminary
924 evaluation of a recombinant circumsporozoite protein vaccine against *Plasmodium*
925 *falciparum* malaria. *New England Journal of Medicine* 336 (1997) 86-91.
- 926 [7] J.A. Regules, S.B. Cicatelli, J.W. Bennett, K.M. Paolino, P.S. Twomey, J.E. Moon, A.K.
927 Kathcart, K.D. Hauns, J.L. Komisar, A.N. Qabar, S.A. Davidson, S. Dutta, M.E.
928 Griffith, C.D. Magee, M. Wojnarski, J.R. Livezey, A.T. Kress, P.E. Waterman, E.
929 Jongert, U. Wille-Reece, W. Volkmuth, D. Emerling, W.H. Robinson, M. Lievens, D.
930 Morelle, C.K. Lee, B. Yassin-Rajkumar, R. Weltzin, J. Cohen, R.M. Paris, N.C.
931 Waters, A.J. Birkett, D.C. Kaslow, W.R. Ballou, C.F. Ockenhouse, and J. Vekemans,
932 Fractional Third and Fourth Dose of RTS,S/AS01 Malaria Candidate Vaccine: A
933 Phase 2a Controlled Human Malaria Parasite Infection and Immunogenicity Study. *J*
934 *Infect Dis* 214 (2016) 762-71.
- 935 [8] S. Chaudhury, J.A. Regules, C.A. Darko, S. Dutta, A. Wallqvist, N.C. Waters, E. Jongert,
936 F. Lemiale, and E.S. Bergmann-Leitner, Delayed fractional dose regimen of the
937 RTS,S/AS01 malaria vaccine candidate enhances an IgG4 response that inhibits
938 serum opsonophagocytosis. *Sci Rep* 7 (2017) 7998.
- 939 [9] S. Pallikkuth, S. Chaudhury, P. Lu, L. Pan, E. Jongert, U. Wille-Reece, and S. Pahwa, A
940 delayed fractionated dose RTS,S AS01 vaccine regimen mediates protection via
941 improved T follicular helper and B cell responses. *Elife* 9 (2020).
- 942 [10] J. Das, J.K. Fallon, T.C. Yu, A. Michell, T.J. Suscovich, C. Linde, H. Natarajan, J.
943 Weiner, M. Coccia, S. Gregory, M.E. Ackerman, E. Bergmann-Leitner, L. Fontana, S.
944 Dutta, D.A. Lauffenburger, E. Jongert, U. Wille-Reece, and G. Alter, Delayed
945 fractional dosing with RTS,S/AS01 improves humoral immunity to malaria via a
946 balance of polyfunctional NANP6- and Pf16-specific antibodies. *Med (N Y)* 2 (2021)
947 1269-1286 e9.
- 948 [11] M.M. Hou, J.R. Barrett, Y. Themistocleous, T.A. Rawlinson, A. Diouf, F.J. Martinez,
949 C.M. Nielsen, A.M. Lias, L.D.W. King, N.J. Edwards, N.M. Greenwood, L. Kingham,
950 I.D. Poulton, B. Khozoe, C. Goh, D.J. Mac Lochlainn, J. Salkeld, M. Guilotte-
951 Blisnick, C. Huon, F. Mohring, J.M. Reimer, V.S. Chauhan, P. Mukherjee, S. Biswas,
952 I.J. Taylor, A.M. Lawrie, J.S. Cho, F.L. Nugent, C.A. Long, R.W. Moon, K. Miura, S.E.
953 Silk, C.E. Chitnis, A.M. Minassian, and S.J. Draper, Impact of a blood-stage vaccine
954 on *Plasmodium vivax* malaria. *medRxiv* (2022).
- 955 [12] C.M. Nielsen, A. Ogbe, I. Pedroza-Pacheco, S.E. Doeleman, Y. Chen, S.E. Silk, J.R.
956 Barrett, S.C. Elias, K. Miura, A. Diouf, M. Bardelli, R.A. Dabbs, L. Barfod, C.A. Long,
957 B.F. Haynes, R.O. Payne, A.M. Minassian, T. Bradley, S.J. Draper, and P. Borrow,
958 Protein/AS01B vaccination elicits stronger, more Th2-skewed antigen-specific human
959 T follicular helper cell responses than heterologous viral vectors. *Cell Rep Med* 2
960 (2021) 100207.
- 961 [13] K.M. Kwiatkowska, C.G. Mkindi, and C.M. Nielsen, Human lymphoid tissue sampling for
962 vaccinology. *Front Immunol* 13 (2022) 1045529.
- 963 [14] A. Nicolas, G. Sannier, M. Dube, M. Nayrac, A. Tauzin, M.M. Painter, R.R. Goel, M.
964 Laporte, G. Gendron-Lepage, H. Medjahed, J.C. Williams, N. Brassard, J. Niessl, L.
965 Gokool, C. Morrisseau, P. Arlotto, C. Tremblay, V. Martel-Laferrriere, A. Finzi, A.R.
966 Greenplate, E.J. Wherry, and D.E. Kaufmann, An extended SARS-CoV-2 mRNA
967 vaccine prime-boost interval enhances B cell immunity with limited impact on T cells.
968 *iScience* 26 (2023) 105904.
- 969 [15] G. Arumugakani, S.J. Stephenson, D.J. Newton, A. Rawstron, P. Emery, G.M. Doody,
970 D. McGonagle, and R.M. Tooze, Early Emergence of CD19-Negative Human
971 Antibody-Secreting Cells at the Plasmablast to Plasma Cell Transition. *J Immunol*
972 198 (2017) 4618-4628.
- 973 [16] H.E. Mei, I. Wirries, D. Frolich, M. Brisslert, C. Giesecke, J.R. Grun, T. Alexander, S.
974 Schmidt, K. Luda, A.A. Kuhl, R. Engelmann, M. Durr, T. Scheel, M. Bokarewa, C.
975 Perka, A. Radbruch, and T. Dorner, A unique population of IgG-expressing plasma
976 cells lacking CD19 is enriched in human bone marrow. *Blood* 125 (2015) 1739-48.

- 977 [17] J.L. Halliley, C.M. Tipton, J. Liesveld, A.F. Rosenberg, J. Darce, I.V. Gregoretti, L.
978 Popova, D. Kaminiski, C.F. Fucile, I. Albizua, S. Kyu, K.Y. Chiang, K.T. Bradley, R.
979 Burack, M. Slifka, E. Hammarlund, H. Wu, L. Zhao, E.E. Walsh, A.R. Falsey, T.D.
980 Randall, W.C. Cheung, I. Sanz, and F.E. Lee, Long-Lived Plasma Cells Are
981 Contained within the CD19(-)CD38(hi)CD138(+) Subset in Human Bone Marrow.
982 *Immunity* 43 (2015) 132-45.
- 983 [18] D.C. Nguyen, C.J. Joyner, I. Sanz, and F.E. Lee, Factors Affecting Early Antibody
984 Secreting Cell Maturation Into Long-Lived Plasma Cells. *Front Immunol* 10 (2019)
985 2138.
- 986 [19] A. Tomic, I. Tomic, Y. Rosenberg-Hasson, C.L. Dekker, H.T. Maecker, and M.M. Davis,
987 SIMON, an Automated Machine Learning System, Reveals Immune Signatures of
988 Influenza Vaccine Responses. *J Immunol* 203 (2019) 749-759.
- 989 [20] C. Nielsen, J. Barrett, C. Davis, J. Fallon, C. Goh, A. Michell, C. Griffin, A. Kwok, C.
990 Loos, S. Darko, F. Laboune, S. Silk, M. Tekman, J. Francica, A. Ransier, R. Payne,
991 A. Minassian, D. Lauffenburger, R. Seder, D. Douek, G. Alter, and S. Draper,
992 Delayed booster dosing improves human antigen-specific Ig and B cell responses to
993 the RH5.1/AS01_B malaria vaccine. *medRxiv* (2022) 2022.04.25.22274161.
- 994 [21] K. Miura, A.C. Orcutt, O.V. Muratova, L.H. Miller, A. Saul, and C.A. Long, Development
995 and characterization of a standardized ELISA including a reference serum on each
996 plate to detect antibodies induced by experimental malaria vaccines. *Vaccine* 26
997 (2008) 193-200.
- 998 [22] R.O. Payne, S.E. Silk, S.C. Elias, K. Miura, A. Diouf, F. Galaway, H. de Graaf, N.J.
999 Brendish, I.D. Poulton, O.J. Griffiths, N.J. Edwards, J. Jin, G.M. Labbe, D.G. Alanine,
1000 L. Siani, S. Di Marco, R. Roberts, N. Green, E. Berrie, A.S. Ishizuka, C.M. Nielsen,
1001 M. Bardelli, F.D. Partey, M.F. Ofori, L. Barfod, J. Wambua, L.M. Murungi, F.H. Osier,
1002 S. Biswas, J.S. McCarthy, A.M. Minassian, R. Ashfield, N.K. Viebig, F.L. Nugent,
1003 A.D. Douglas, J. Vekemans, G.J. Wright, S.N. Faust, A.V. Hill, C.A. Long, A.M.
1004 Lawrie, and S.J. Draper, Human vaccination against RH5 induces neutralizing
1005 antimalarial antibodies that inhibit RH5 invasion complex interactions. *JCI Insight* 2
1006 (2017).
- 1007 [23] A.D. Douglas, N.J. Edwards, C.J. Duncan, F.M. Thompson, S.H. Sheehy, G.A. O'Hara,
1008 N. Anagnostou, M. Walther, D.P. Webster, S.J. Dunachie, D.W. Porter, L. Andrews,
1009 S.C. Gilbert, S.J. Draper, A.V. Hill, and P. Bejon, Comparison of modeling methods
1010 to determine liver-to-blood inocula and parasite multiplication rates during controlled
1011 human malaria infection. *J Infect Dis* 208 (2013) 340-5.
- 1012 [24] A.M. Minassian, Y. Themistocleous, S.E. Silk, J.R. Barrett, A. Kemp, D. Quinkert, C.M.
1013 Nielsen, N.J. Edwards, T.A. Rawlinson, F. Ramos Lopez, W. Roobsoong, K.J. Ellis,
1014 J.S. Cho, E. Aunin, T.D. Otto, A.J. Reid, F.A. Bach, G.M. Labbe, I.D. Poulton, A.
1015 Marini, M. Zaric, M. Mulatier, R. Lopez Ramon, M. Baker, C.H. Mitton, J.C. Sousa, N.
1016 Rachaphaew, C. Kumpitak, N. Maneechai, C. Suansomjit, T. Piteekan, M.M. Hou, B.
1017 Khozoe, K. McHugh, D.J. Roberts, A.M. Lawrie, A.M. Blagborough, F.L. Nugent, I.J.
1018 Taylor, K.J. Johnson, P.J. Spence, J. Sattabongkot, S. Biswas, J.C. Rayner, and S.J.
1019 Draper, Controlled human malaria infection with a clone of *Plasmodium vivax* with
1020 high-quality genome assembly. *JCI Insight* 6 (2021).
1021